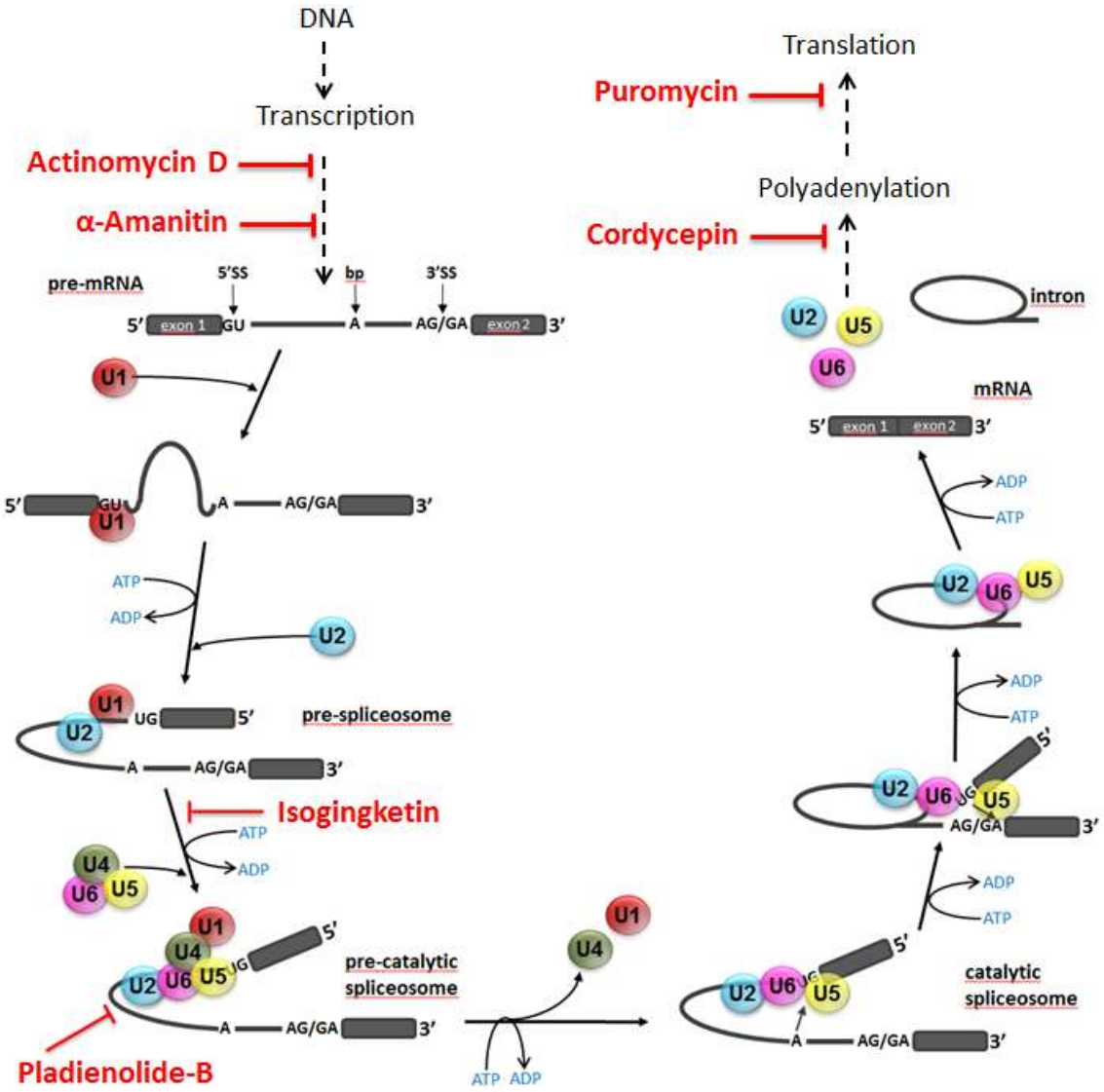

Supplementary Figure 1. Schematic diagram of the transcriptional process, including assembly process of the spliceosome, and inhibitor compounds that were used to block the respective steps (data in Fig. 1B, 1C, 1D and Supplementary Figure 2).

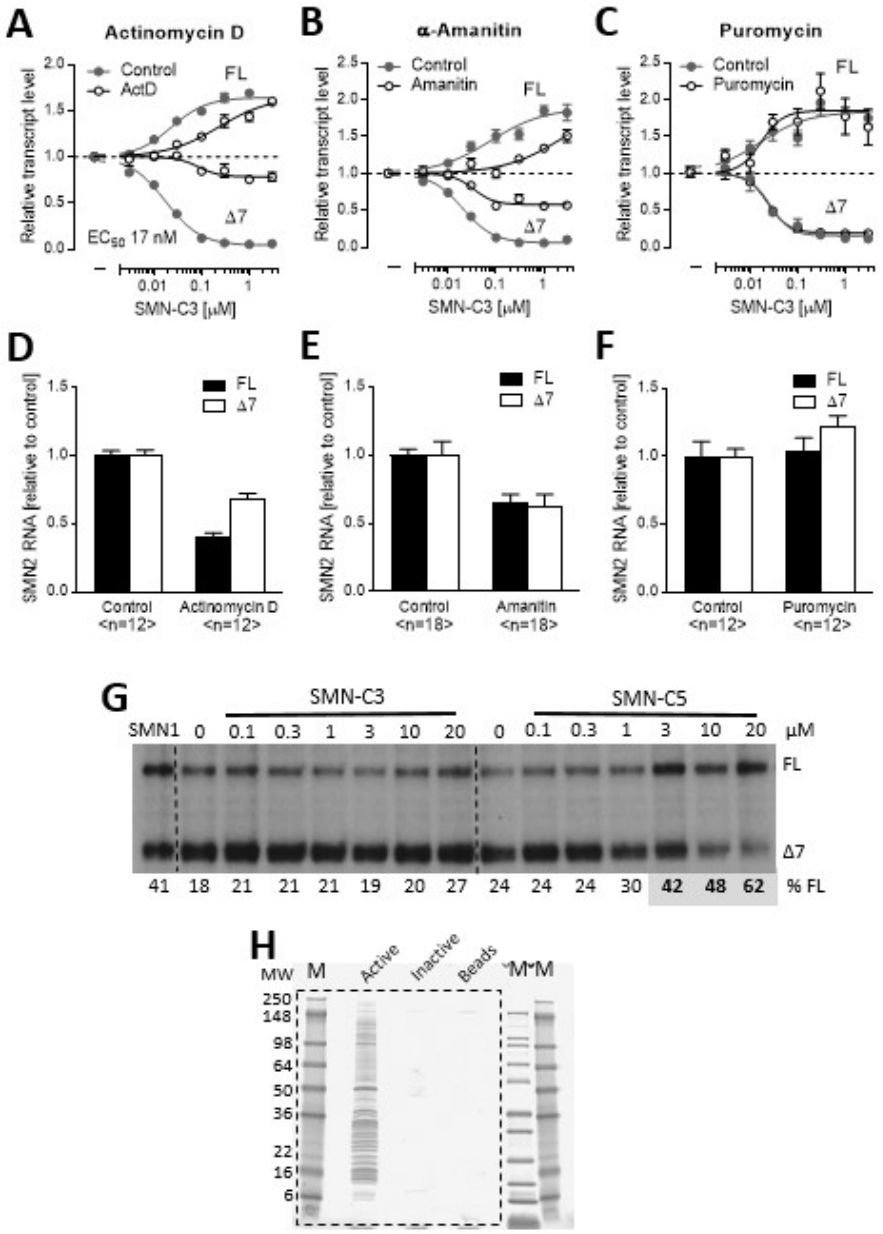

Supplementary Figure 2. Compound effect on transcription, translation and RNA splicing

RT-PCR analysis of *SMN2* mRNA FL and Δ7 relative transcripts levels in SMA Type I patient fibroblasts treated for 6 hours with inhibitors acting at various steps of transcription or translation (**A**) actinomycin D (1 µg/ml), (**B**) α-amanitin (50 µg/ml), and (**C**) puromycin (10 µg/ml), and simultaneously treated with the *SMN2* splicing modifier SMN-C3. (**D**, **E**, **F**) Baseline amounts of SMN2 FL or Δ7 mRNA after 6 hours treatment with (**D**) actinomycin D (1 µg/ml), (**E**) α-amanitin (50 µg/ml), and (**F**) puromycin (10 µg/ml). (**G**) In vitro splicing assay of SMN2-minigene transcript with cell-free nuclear extract, in the presence of SMN-C3 and SMN-C5 (0.1-20 µM). Splicing of SMN1 minigene transcript served as a control in lane 1. (**H**) Full commassie gel of Fig. 1D wish the dashed line illustrating the region shown in the main Figure. "M" indicated Marker. Data in (**A-F**) represent means ± SEM of 12-18 assessments per concentration in up to 6 independent experiments, data in (**G**) are representative of three independent experiments.

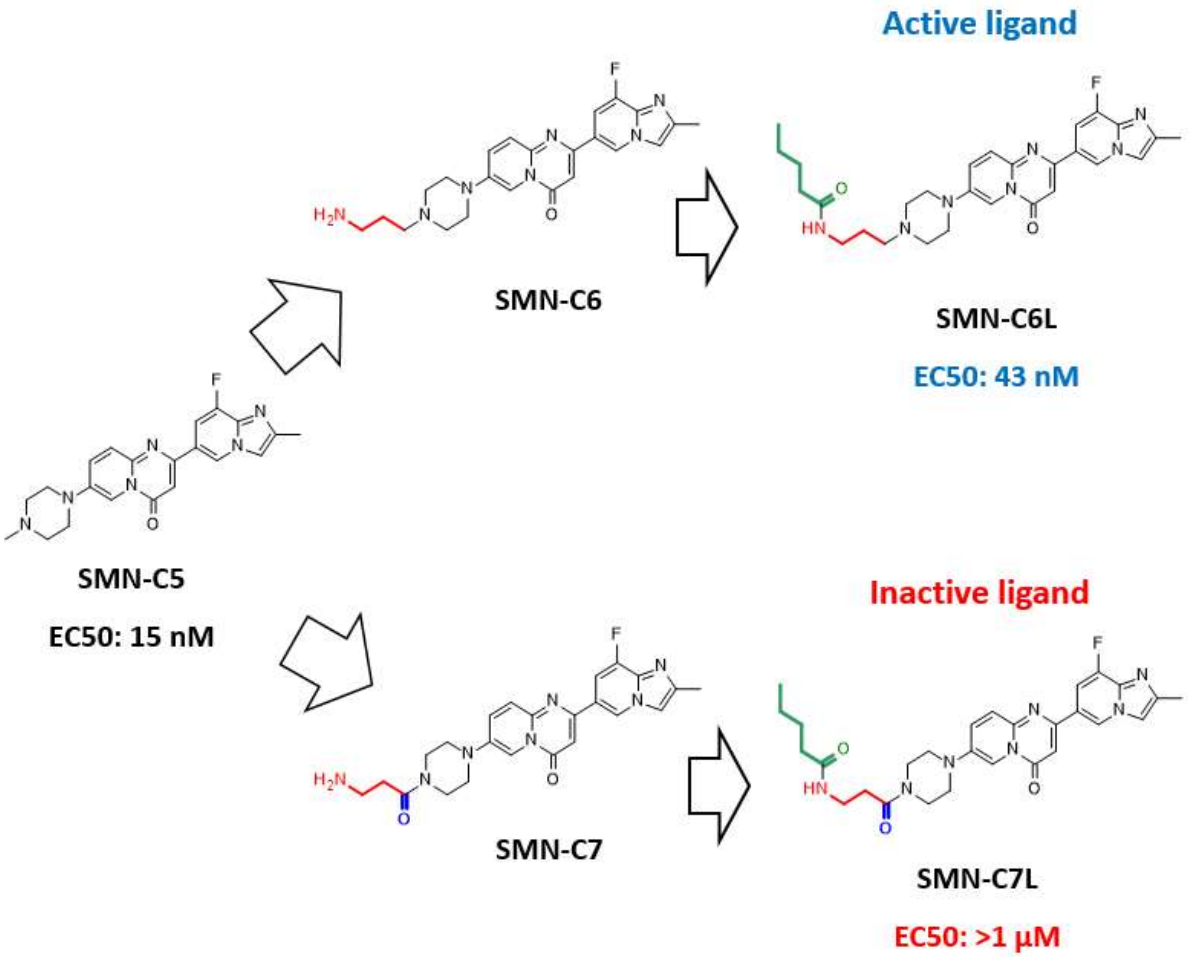

Supplementary Figure 3. Schematic representation of ligand generation starting with SMN-C5, a highly potent *SMN2* splicing modifier

By minimal modification, two ligands were created, SMN-C6 and SMN-C7. SMN-C6L and SMN-C7L were synthesized to mimic the immobilization of the later and were tested to verify potency in modifying *SMN2* splicing in a cellular assay using Type I patient fibroblasts (SMN-C6L, Active, EC50 43 nM; SMN-C7L, Inactive, EC50 >1 µM)

A

Gene names	sn RNP	Active/Inactive (log 2 Fold change)
SNRPD1	Sm protein	3.92
SNRPD2	Sm protein	3.13
SNRPD3	Sm protein	3.96
SNRPE	Sm protein	3.92
SNRPF	Sm protein	3.90
SNRPA	U1	3.70
SNRNP70	U1	3.70
SRSF1 ASF SF2	U1 /U2	3.84
U2AF2 U2AF65	U2	2.80
SF3B1	U2	3.20
SF3B3	U2	2.29
PTBP1 PTB	U2	3.92
PRPF8	U5	2.07
EFTUD2	U5	2.91
DHX15	U2; U5; U6	3.90
NHP2L1	U4/U6-U5	4.89
SART3	U6	2.63
SRPK2	U4/U6-U5	3.96
NONO	U4/U6-U6/U1A	2.98
SFPQ PSF	U4/U6-U7/U1A	3.49

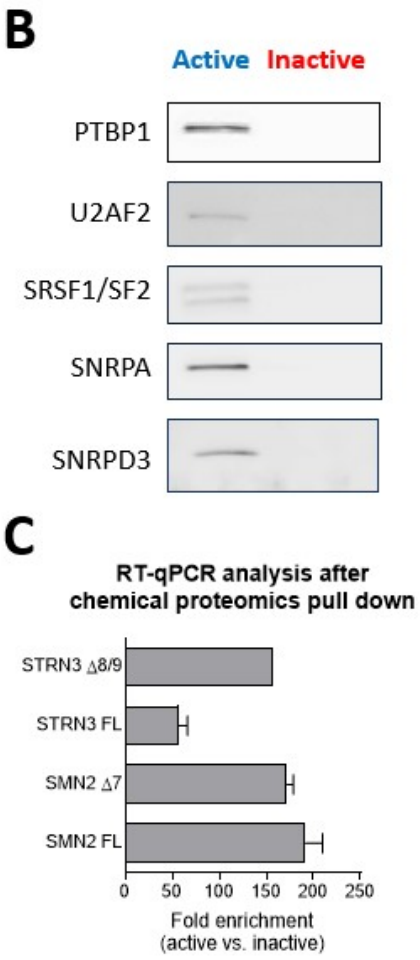

Supplementary Figure 4. Chemical proteomics using either splicing modifiers as ligands immobilized on sepharose beads

Whole protein extracts from differentially labeled SMA type 1 patient fibroblasts were loaded either on Active (SMN-C6) or Inactive (SMN-C7) affinity matrices. Elution fractions from both affinity chromatographies were combined, separated by one-dimensional gel electrophoresis, in gel digested and peptides extracted followed by LC-MS/MS analysis and quantification (**A**) Representation of some members of the snRNP family and levels of enrichment in the chemical proteomics pull-down with Active vs. Inactive compound (indicated by log 2-fold change). (**B**) Western blot analysis of the pull-down to Active vs. Inactive compound with antibodies against PTBP1, U2AF2, SRSF1/SF2, SNRPA and SNRPD3. (**C**) Fold enrichment (Active over Inactive compound) of *SMN2* and *STRN3* mRNA variants in eluates of the affinity matrices on immobilized active vs. inactive compound. Data in (**C**) represent means ±SEM of three independent samples.

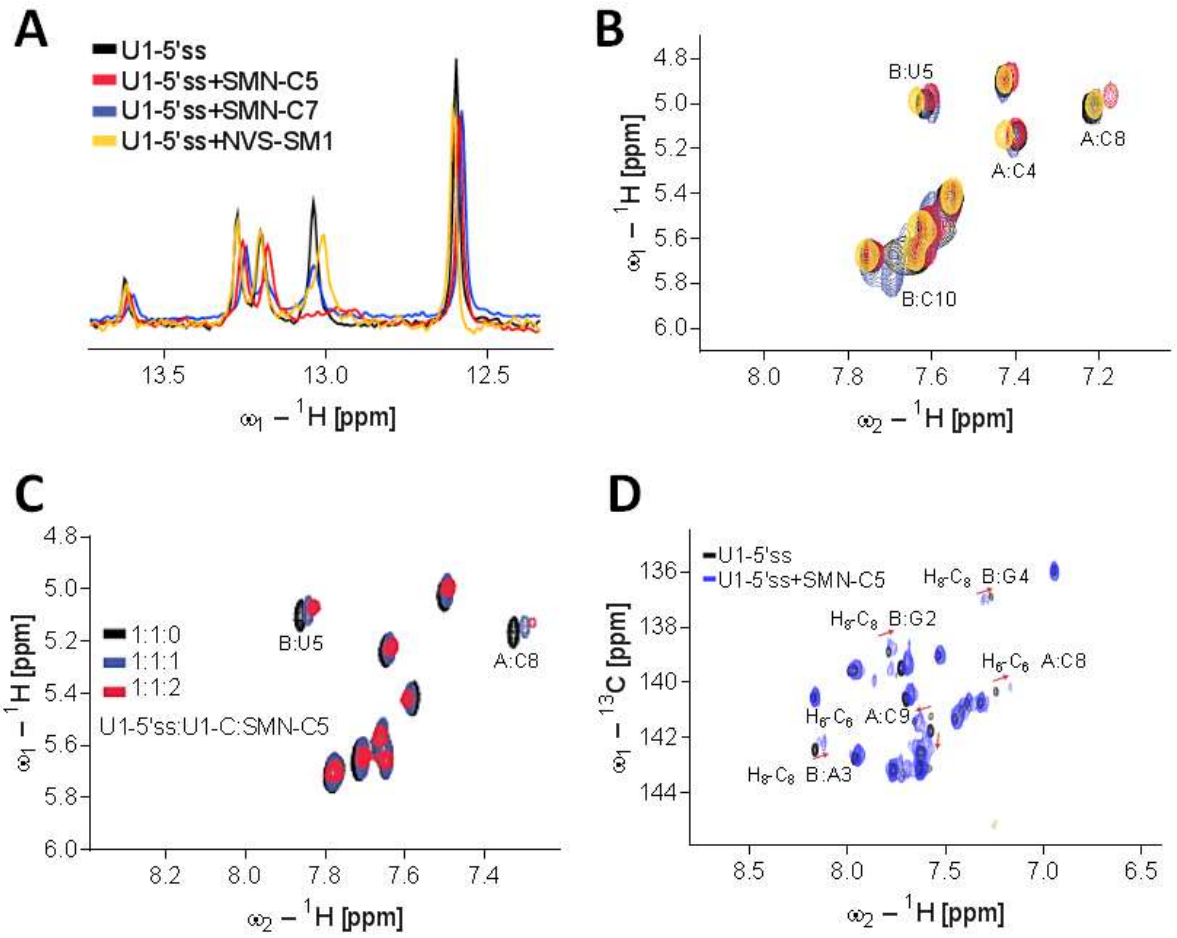

Supplementary Figure 5. NMR spectra of the binding of splicing modifiers to U1-5'ss RNA duplex

(**A**) Overlay of the 1D ^{1}H NMR spectra showing the signal of the imino protons of the RNA duplex (U1-5'ss) upon addition of the three different compounds (SMN-C5/active, SMN-C7/inactive, and NVS-SM1). (**B**) Overlay of the 2D ^{1}H-^{1}H TOCSY spectra showing the signal of the pyrimidine bases of the RNA duplex (U1-5'ss) upon addition of the three different compounds (SMN-C5/active, SMN-C7/inactive, and NVS-SM1). (**C**) NMR titration performed in presence of the zinc finger domain of U1-C supports SMN-C5 binding in the same location without affecting the binding of U1-C, both binding interfaces are located on opposite sites around the invariant GU motif of the 5'ss. (**D**) Overlay of the 2D ^{13}C-^{1}H HSQC of the RNA duplex recorded before and after addition of SMN-C5. Protons that experienced large chemical shift changes are located in the major groove of the RNA duplex.

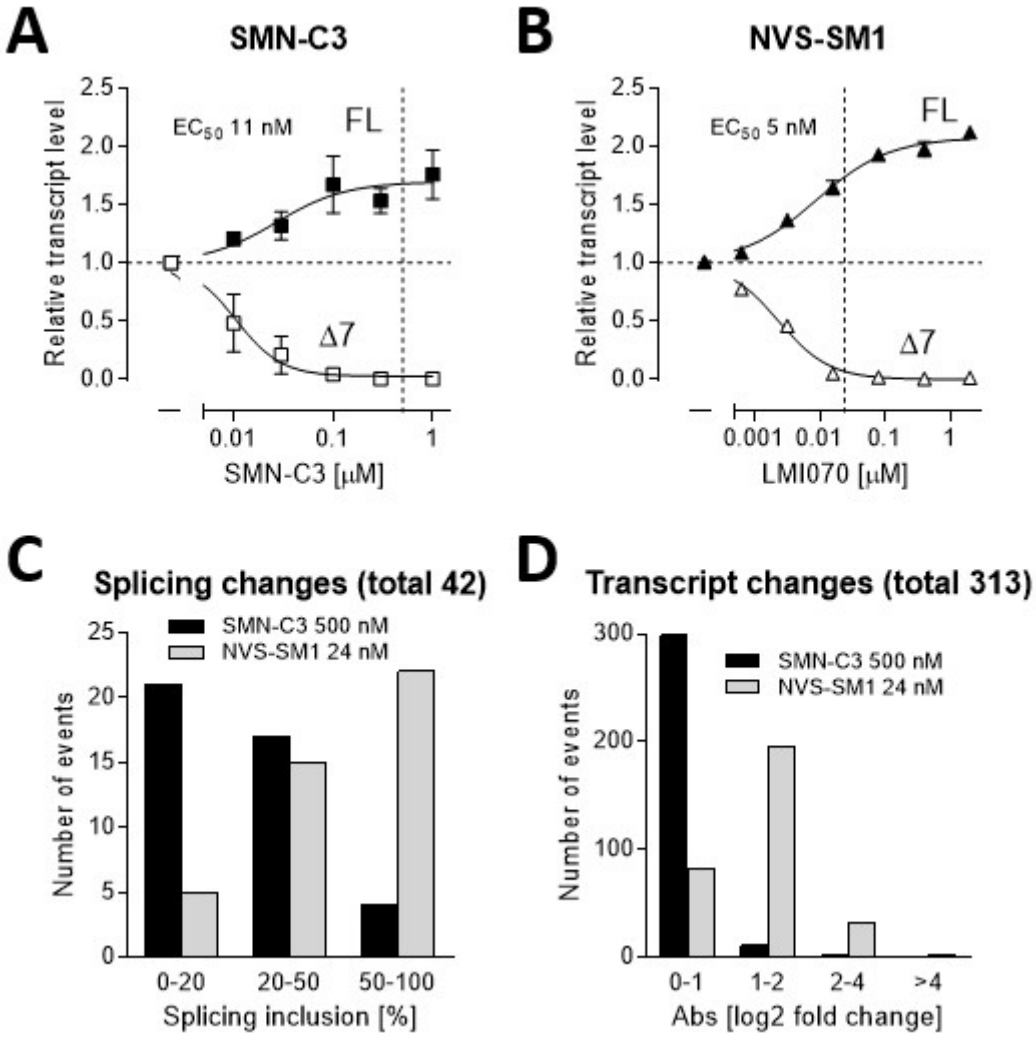

Supplementary Figure 6. Comparison of splicing correction, total number of splicing and transcript changes

RT-PCR analysis of *SMN2* full-length (FL) and exon 7 lacking (Δ7) mRNA in type 1 SMA patient fibroblasts treated with SMN-C3 (**A**) at 500 nM (~50x EC_{50}), and NVS-SM1 (**B**) at 24 nM (~5x EC_{50}, respectively), indicated by the dashed lines. (C) Histogram of transcriptome-wide splicing events (total 42) for all treatment conditions with a ΔPSI of >0.4 (SMN-C3 500 nM; NVS-SM1 24 nM), with binning at the 20% and 50% splicing correction level. (**D**) Histogram of transcriptional profiling changes (total 437) at $p<0.001$ in any of the treatment conditions, with binning at the 1, 2 and 4 fold change level. For SMN-C3, 95% of the log fold changes were <1.

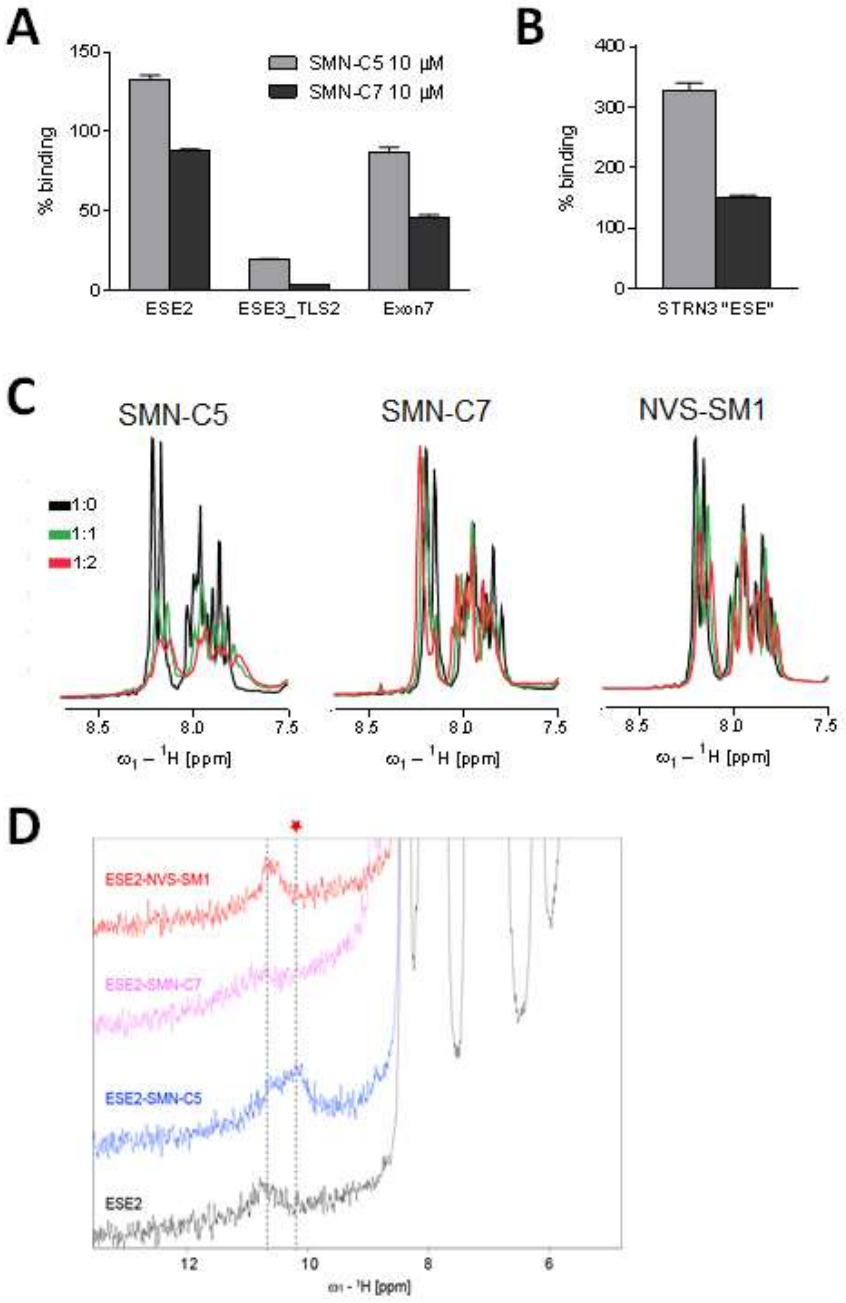

Supplementary Figure 7. Binding of the splicing modifiers to RNA measured by SPR and solution NMR

SPR (Biacore) binding at a single concentration 10µM with the active compound, SMN-C5, and the inactive compound SMN-C7 to ESE2 in *SMN2* exon 7 (**A**) or to the putative ESE in *STRN3* exon 8 (**B**). (**C**) Binding of SMN-C5, SMN-C7 and NVS-SM1 to *SMN2* ESE2 RNA by means of solution NMR. **(D)** Addition of SMN-C5 but not SMN-C7 or NVS-SM1 induced the formation of new broad imino signals (asterisk) in the proton 1D spectrum of the complex ESE2-SMN-C5, Data in (**A**) and (**B**) represent means ± SEM of three replicates.

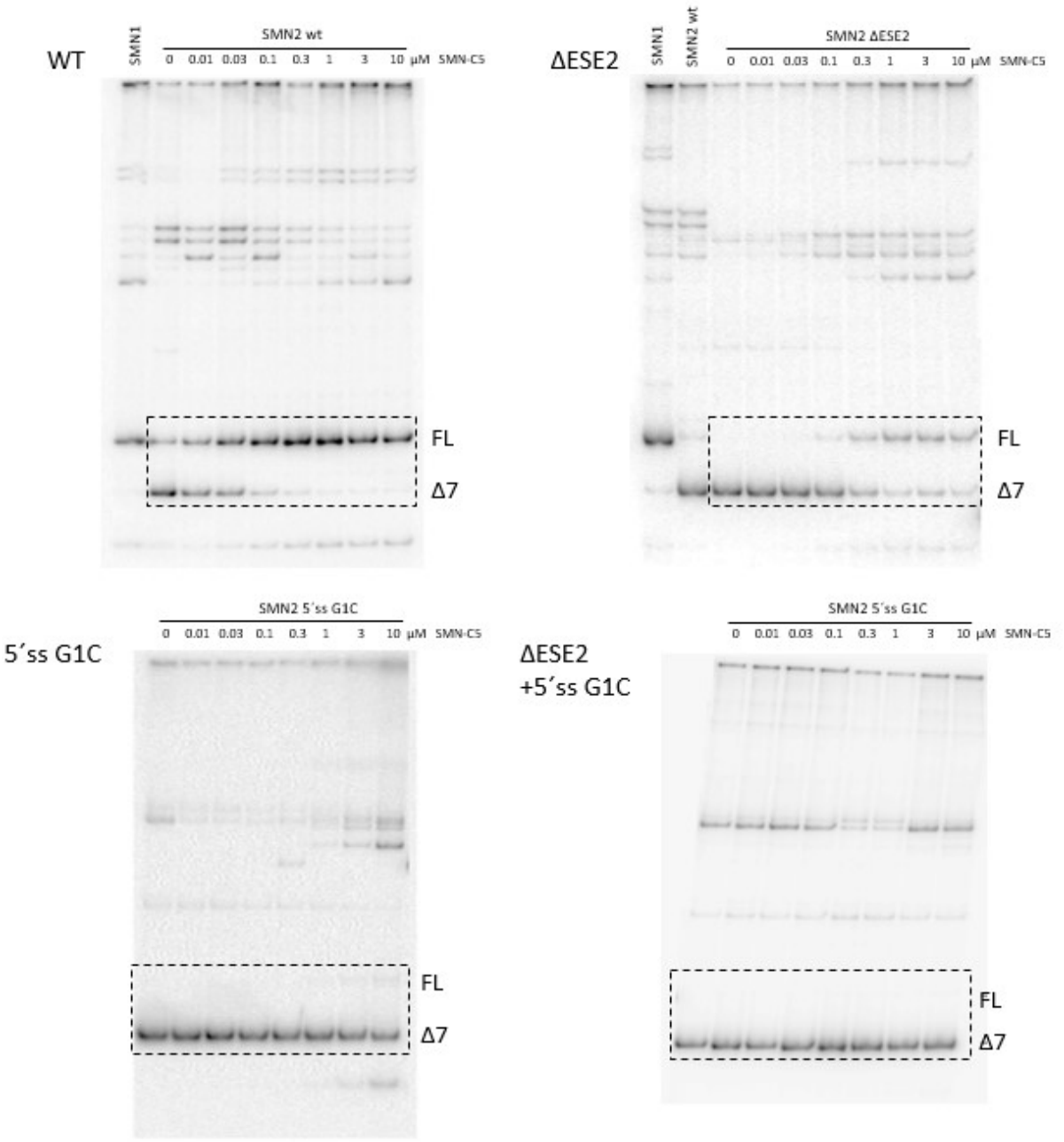

Supplementary Figure 8. Full blot pictures from Fig. 5A

Shown are full scans of the blots illustrated in Fig. 5A (Upper left: SMN2 wt; Upper right: SMN2 ΔESE2; Lower left: SMN2 5´ss G1C; Lower right: SMN2 ΔESE2+5´ss G1C). Dashed areas indicate the region shown in the main Figure.

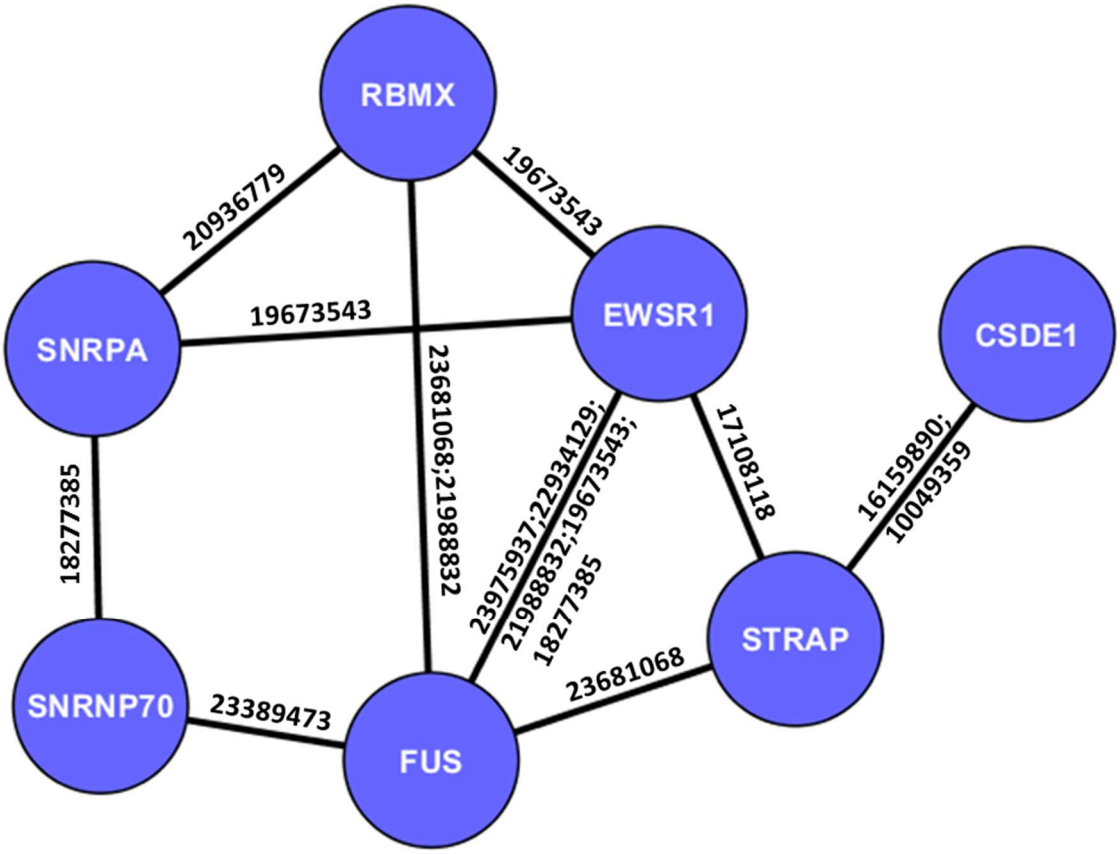

Supplementary Figure 9. Chemoproteomics and Protein pull down analysis with ESE2 construct

In nuclear extracts of SMA type 1 patient fibroblasts, pull downs were performed using ESE2 as bait. Out of 821 proteins identified, SMN-C6 specifically induced the binding of 10 proteins to ESE2 (pVal<0.05; unique peptides >1) which were not observed in the presence of the inactive compound SMN-C7. Based on String functional protein association analysis (string.db.org; high confidence 0.7), 7 of these proteins are described to be part of a complex: the U1 snRNP proteins A and 70; hnRNP G (also known as RBMX), FUS, EWSR1, STRAP, CSDE1. Numbers at the edges of the diagram indicate PubMed identifiers supporting the respective interactions.

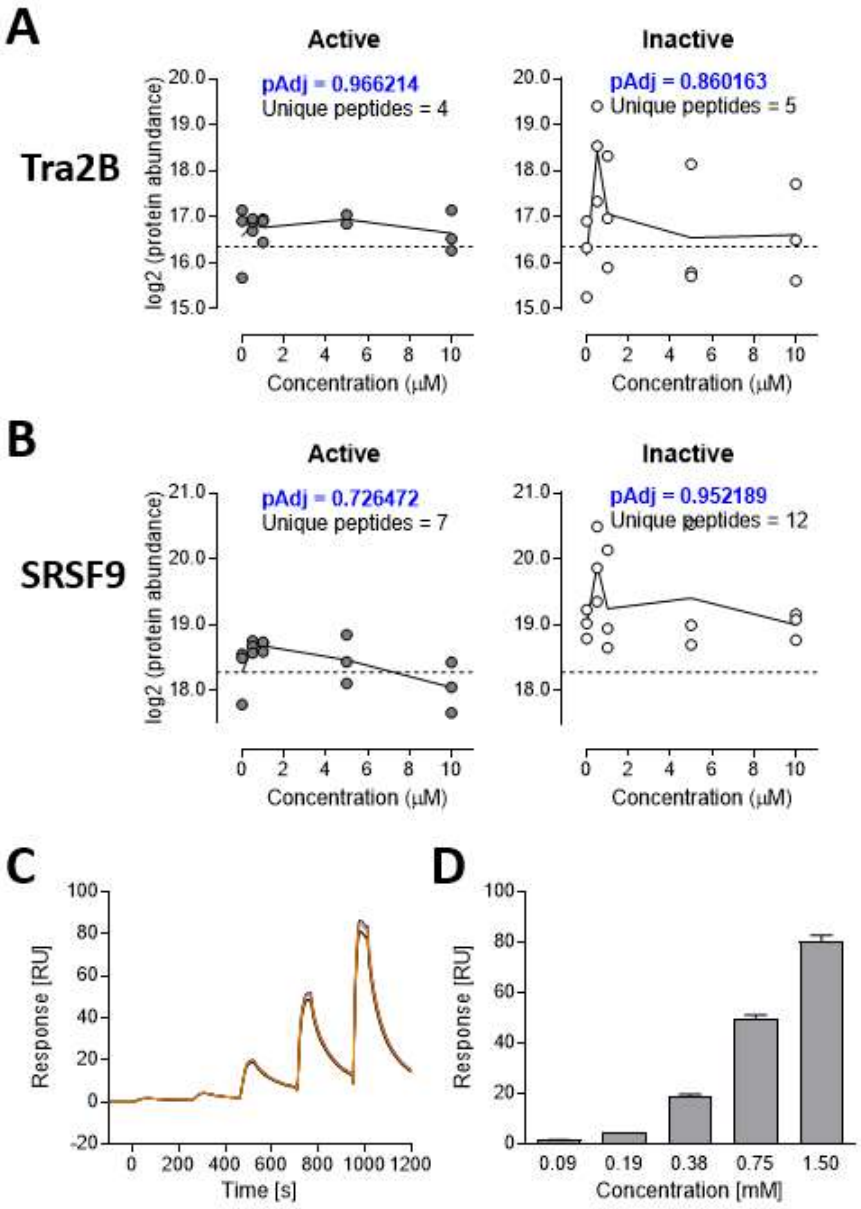

Supplementary Figure 10. Affinity Pull down enrichment of Tra2B and SRSF9 and Surface Plasmon Resonance of hnRNPG binding

(**A**) Protein abundance (log2) of Tra2B after affinity enrichment with the SMN2 ESE2 RNA sequence as bait, in the presence of Active (SMN-C6) or Inactive (SMN-C7) ligand. (**B**) Protein abundance (log2) of SRSF9 after affinity enrichment with the SMN2 ESE2 RNA sequence as bait, in the presence of increasing concentrations of Active (SMN-C6) or Inactive (SMN-C7) ligand. (**C**) SPR titration of hnRNPG (in quadruplicate) at 0.094-1.5 μM over immobilized ESE2 surface. Biotinylated ESE2 was immobilized on streptavidin surface on CAP sensor to densities of ~20 RU. Saturation of SPR signal for hnRNP G could not be achieved due to non-specific binding of hnRNP G onto sensor surface at concentrations higher than 1.5 μM. (**D**) Quantitative assessment of SPR signals monitored in (**C**). SPR signal amplitude was measured in the middle of the association phase. Data in (**D**) represent mean ± SEM of four independent experiments.

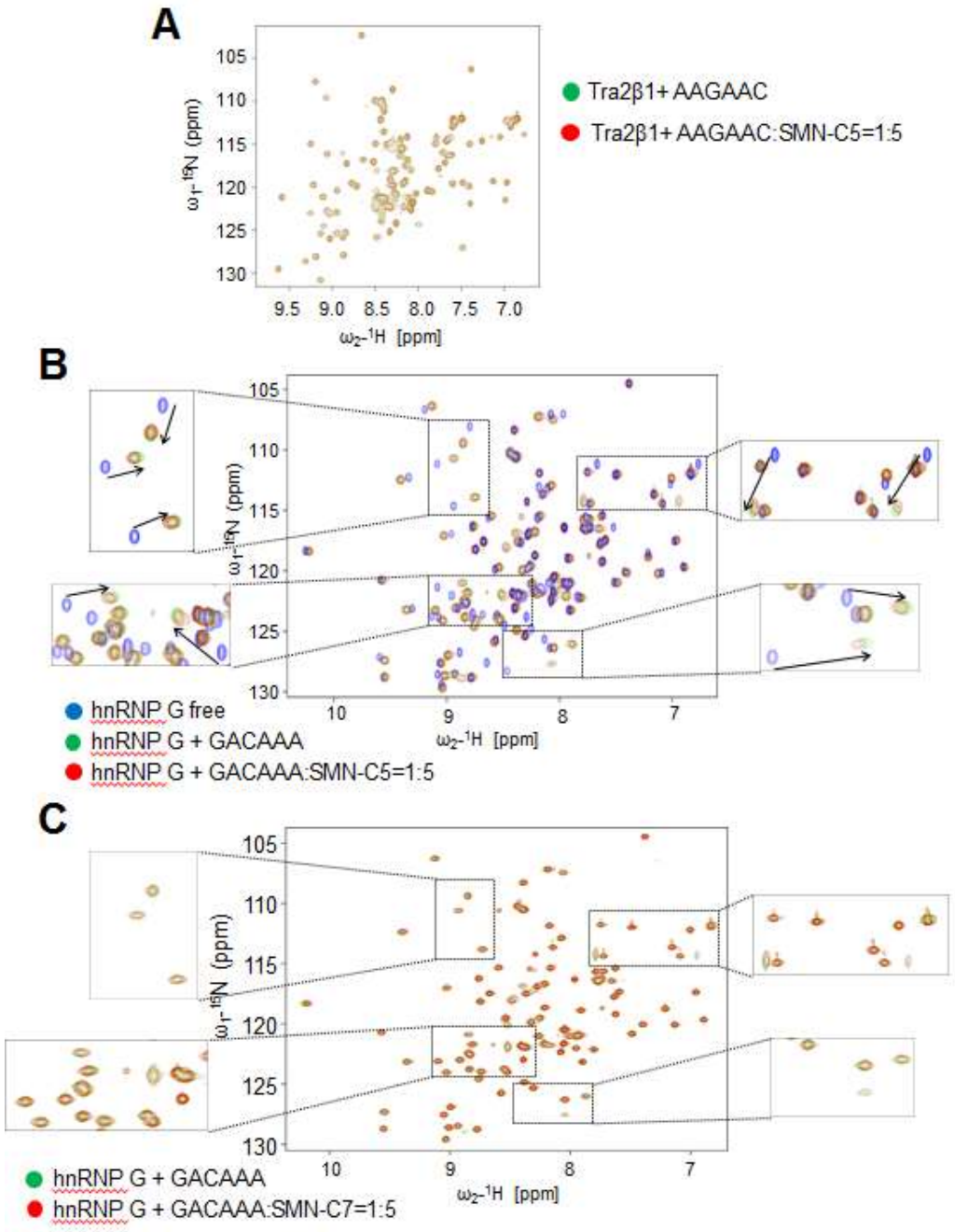

Supplementary Figure 11. Solution NMR binding of SMN-C5 to several protein-RNA complexes involved in *SMN2* splicing

(**A**) No chemical shift perturbations were observed when Tra2-β1 RRM in complex with RNA was titrated with SMN-C5 up to five fold in excess, indicating that SMN-C5 does not affect the interaction between Tra2-β1 and RNA. (**B**) In contrast, chemical shift perturbations were observed when hnRNP G RRM bound to RNA was titrated with SMN-C5. These perturbations were in the direction of the free form protein indicating that the compound destabilizes the interaction of hnRNP G RRM with the RNA. (**C**) The absence of chemical shift perturbation with the inactive compound SMN-C7 indicated that the effect of SMN-C5 observed on hnRNP G is specific.

Supplementary Tables:

Accession	Entry	Gene names	fold change active/inactive	adjusted p-value
ABCF1_HUMAN	Q8NE71	ABCF1 ABC50	8,0	1,900E-08
ABCF2_HUMAN	Q9UG63	ABCF2 HUSSY-18	21,0	8,930E-09
ACOT9_HUMAN	Q9Y305	ACOT9 CGI-16	13,8	1,020E-08
AGO2_HUMAN	Q9UKV8	AGO2 EIF2C2	12,4	1,727E-04
ANKZ1_HUMAN	Q9H8Y5	ANKZF1 ZNF744	5,8	3,260E-05
ANR17_HUMAN	O75179	ANKRD17 GTAR KIAA0697	11,9	1,720E-06
ANXA1_HUMAN	P04083	ANXA1 ANX1 LPC1	3,5	1,485E-02
ANXA2_HUMAN	P07355	ANXA2 ANX2 ANX2L4 CAL1H LPC2D	5,1	1,020E-06
AP2A1_HUMAN	O95782	AP2A1 ADTAA CLAPA1	4,2	5,190E-05
AP2M1_HUMAN	Q96CW1	AP2M1 CLAPM1 KIAA0109	12,4	3,820E-05
ASCC3_HUMAN	Q8N3C0	ASCC3 HELIC1	5,8	2,707E-04
ASPH_HUMAN	Q12797	ASPH	12,1	5,920E-10
ATD3A_HUMAN	Q9NVI7	ATAD3A	5,2	1,010E-05
BOP1_HUMAN	Q14137	BOP1 KIAA0124	8,1	5,150E-06
BTF3_HUMAN	P20290	BTF3 NACB OK/SW-cl.8	14,6	1,260E-08
C1QBP_HUMAN	Q07021	C1QBP GC1QBP HABP1 SF2P32	6,1	1,300E-07
CA123_HUMAN	Q9NWV4	C1orf123	20,1	1,840E-08
CAPR1_HUMAN	Q14444	CAPRIN1 GPIAP1 GPIP137 M11S1 RNG105	12,8	8,900E-07
CC124_HUMAN	Q96CT7	CCDC124	24,4	1,150E-10
CCD80_HUMAN	Q76M96	CCDC80 DRO1 URB HBE245	3,9	3,934E-03
CDC5L_HUMAN	Q99459	CDC5L KIAA0432 PCDC5RP	9,4	1,640E-09
CG050_HUMAN	Q8WUJ3	CEMIP KIAA1199	21,9	6,650E-10
CH033_HUMAN	Q9BRJ6	C7orf50 FP15621	12,1	2,530E-05
CHD3_HUMAN	Q9H7E9	C8orf33	12,1	1,200E-06
CHD4_HUMAN	Q12873	CHD3	9,9	1,590E-05
CHTOP_HUMAN	Q14839	CHD4	7,7	2,300E-07
CIRBP_HUMAN	Q9Y3Y2	CHTOP C1orf77 FOP HT031 PP7704	15,2	1,650E-08
CKAP4_HUMAN	Q14011	CIRBP A18HNRNP CIRP	15,8	2,180E-10
CN166_HUMAN	Q07065	CKAP4	4,9	3,540E-06
CO1A1_HUMAN	Q9Y224	C14orf166 CGI-99	8,4	2,090E-05
CO1A2_HUMAN	P02452	COL1A1	4,5	9,290E-06
CO6A3_HUMAN	P08123	COL1A2	3,2	7,410E-05
COCA1_HUMAN	P12111	COL6A3	3,2	4,630E-06
COPA_HUMAN	Q99715	COL12A1 COL12A1L	5,2	1,730E-06
CPNE1_HUMAN	P53621	COPA	14,4	1,790E-09
CPNE3_HUMAN	Q99829	CPNE1 CPN1	14,1	6,170E-10
CPNE7_HUMAN	O75131	CPNE3 CPN3 KIAA0636	14,5	5,790E-06
CSDE1_HUMAN	Q9UBL6	CPNE7	13,3	2,090E-08
CTCF_HUMAN	O75534	CSDE1 D1S155E KIAA0885 NRU UNR	15,3	6,250E-07
CYR61_HUMAN	P49711	CTCF	11,7	2,010E-06
DDX1_HUMAN	O00622	CYR61 CCN1 GIG1 IGFBP10	6,3	3,020E-09
DDX17_HUMAN	Q92841	DDX17	13,8	3,100E-10

DDX18_HUMAN	Q9NVP1	DDX18	8,9	3,690E-08
DDX21_HUMAN	Q92499	DDX1	11,8	1,590E-08
DDX24_HUMAN	Q9NR30	DDX21	14,7	2,820E-11
DDX27_HUMAN	Q9GZR7	DDX24	10,8	1,450E-07
DDX3X_HUMAN	Q96GQ7	DDX27 RHLP HSPC259 PP3241	5,8	3,860E-10
DDX5_HUMAN	O00571	DDX3X DBX DDX3	14,8	6,440E-11
DDX50_HUMAN	Q9BQ39	DDX50	8,6	7,480E-08
DDX54_HUMAN	Q8TDD1	DDX54	10,2	1,480E-07
DDX55_HUMAN	Q8NHQ9	DDX55 KIAA1595	7,3	6,480E-07
DDX6_HUMAN	P17844	DDX5 G17P1 HELR HLR1	14,1	5,290E-10
DECR_HUMAN	P26196	DDX6 HLR2 RCK	16,2	3,365E-04
DHX15_HUMAN	Q16698	DECR1 DECR	6,7	4,600E-05
DHX29_HUMAN	O43143	DHX15 DBP1 DDX15	14,9	9,540E-11
DHX30_HUMAN	Q7Z478	DHX29 DDX29	13,9	1,830E-08
DHX57_HUMAN	Q7L2E3	DHX30 DDX30 KIAA0890	10,4	5,360E-09
DHX9_HUMAN	Q6P158	DHX57	7,4	3,040E-09
DJC10_HUMAN	Q08211	DHX9 DDX9 LKP NDH2	5,7	8,130E-06
DJC21_HUMAN	Q8IXB1	DNAJC10 ERDJ5 UNQ495/PRO1012	14,7	4,170E-06
DKC1_HUMAN	Q5F1R6	DNAJC21 DNAJA5	11,1	2,707E-04
DSRAD_HUMAN	O60832	DKC1 NOLA4	9,9	6,770E-09
DX39A_HUMAN	P55265	ADAR ADAR1 DSRAD G1P1 IFI4	7,4	1,450E-07
EBP2_HUMAN	O00148	DDX39A DDX39	34,4	1,640E-08
EF2_HUMAN	Q99848	EBNA1BP2 EBP2	5,5	7,010E-05
EFTU_HUMAN	P13639	EEF2 EF2	21,9	4,990E-08
EIF3A_HUMAN	P49411	TUFM	6,9	2,300E-10
EIF3B_HUMAN	Q14152	EIF3A EIF3S10 KIAA0139	4,3	2,839E-03
EIF3C_HUMAN	P55884	EIF3B EIF3S9	7,0	1,160E-07
EIF3D_HUMAN	Q99613	EIF3C EIF3S8	8,6	2,430E-10
EIF3E_HUMAN	O15371	EIF3D EIF3S7	4,4	5,892E-04
EIF3F_HUMAN	P60228	EIF3E EIF3S6 INT6	6,2	1,103E-03
EIF3I_HUMAN	O00303	EIF3F EIF3S5	7,7	5,950E-10
EIF3L_HUMAN	Q13347	EIF3I EIF3S2 TRIP1	6,2	1,010E-05
ELAV1_HUMAN	Q9Y262	EIF3L EIF3EIP EIF3S6IP HSPC021 HSPC025 MSTP005	16,9	1,120E-09
ERF1_HUMAN	Q15717	ELAVL1 HUR	11,1	3,180E-06
EXOS1_HUMAN	P62495	ETF1 ERF1 RF1 SUP45L1	11,7	1,485E-02
EXOSX_HUMAN	Q9Y3B2	EXOSC1 CSL4 CGI-108	15,3	1,450E-07
F120A_HUMAN	Q01780	EXOSC10 PMSCL PMSCL2 RRP6	14,8	8,440E-10
FA98A_HUMAN	Q9NZB2	FAM120A C9orf10 KIAA0183 OSSA	5,6	3,070E-08
FBN1_HUMAN	Q8NCA5	FAM98A	6,6	3,100E-08
FBRL_HUMAN	P35555	FBN1 FBN	16,0	6,010E-09
FINC_HUMAN	P22087	FBL FIB1 FLRN	6,0	2,780E-08
FLII_HUMAN	P02751	FN1 FN	3,4	1,380E-05
FMR1_HUMAN	Q13045	FLII FLIL	12,2	8,670E-05
FUS_HUMAN	Q06787	FMR1	3,3	1,170E-06
FXR1_HUMAN	P35637	FUS TLS	19,5	1,080E-09
FXR2_HUMAN	P51114	FXR1	7,2	9,380E-07

G3BP1_HUMAN	P51116	FXR2 FMR1L2	6,2	5,790E-06
G3BP2_HUMAN	Q13283	G3BP1 G3BP	14,1	4,500E-06
GAR1_HUMAN	Q9UN86	G3BP2 KIAA0660	10,1	1,680E-06
GBLP_HUMAN	Q9NY12	GAR1 NOLA1	12,0	6,790E-06
GELS_HUMAN	P63244	GNB2L1 HLC7 PIG21	2,9	1,607E-04
GNL1_HUMAN	P06396	GSN	5,1	7,840E-06
GNL3_HUMAN	P36915	GNL1 HSR1	18,2	5,810E-10
GREM1_HUMAN	Q9BVP2	GNL3 E2IG3 NS	13,8	1,670E-07
GRP78_HUMAN	O60565	GREM1 CKTSF1B1 DAND2 DRM PIG2	4,0	1,010E-05
GRSF1_HUMAN	P11021	HSPA5 GRP78	12,5	1,160E-08
GRWD1_HUMAN	Q12849	GRSF1	14,1	5,640E-10
GSCR2_HUMAN	Q9BQ67	GRWD1 GRWD KIAA1942 WDR28	8,4	1,781E-03
H13_HUMAN	Q9NZM5	GLTSCR2	22,1	2,830E-08
H15_HUMAN	P16402	HIST1H1D H1F3	30,2	6,300E-08
H1X_HUMAN	P16401	HIST1H1B H1F5	22,0	4,670E-08
H2A1A_HUMAN	Q92522	H1FX	29,0	5,950E-10
H2A1B_HUMAN	Q96QV6	HIST1H2AA H2AFR	36,2	2,300E-10
H2A1D_HUMAN	P04908	HIST1H2AB H2AFM; HIST1H2AE H2AFA	29,9	1,440E-10
H2AY_HUMAN	P20671	HIST1H2AD H2AFG	57,4	1,984E-03
H31_HUMAN	O75367	H2AFY MACROH2A1	27,1	2,300E-07
H4_HUMAN	P68431	HIST1H3A H3FA	32,7	3,990E-10
HCD2_HUMAN	P62805	HIST1H4A H4/A H4FA	11,7	2,181E-03
HERC2_HUMAN	Q99714	HSD17B10 ERAB HADH2 MRPP2 SCHAD XH98G2	6,8	2,348E-03
HNRDL_HUMAN	O95714	HERC2	13,5	7,850E-10
HNRH1_HUMAN	O14979	HNRNPDL HNRPDL JKTBP	8,8	1,260E-08
HNRH2_HUMAN	P31943	HNRNPH1 HNRPH HNRPH1	11,4	3,010E-09
HNRH3_HUMAN	P55795	HNRNPH2 FTP3 HNRPH2	13,1	2,180E-09
HNRL1_HUMAN	P31942	HNRNPH3 HNRPH3	12,8	1,780E-09
HNRL2_HUMAN	Q9BUJ2	HNRNPUL1 E1BAP5 HNRPUL1	11,5	1,960E-11
HNRPC_HUMAN	Q1KMD3	HNRNPUL2 HNRPUL2	12,2	9,940E-10
HNRPD_HUMAN	P07910	HNRNPC HNRPC	12,1	1,490E-09
HNRPF_HUMAN	Q14103	HNRNPD AUF1 HNRPD	8,5	2,568E-03
HNRPK_HUMAN	P52597	HNRNPF HNRPF	15,7	7,650E-11
HNRPL_HUMAN	P61978	HNRNPK HNRPK	13,9	5,460E-11
HNRPM_HUMAN	P14866	HNRNPL HNRPL P/OKcl.14	15,7	7,500E-12
HNRPQ_HUMAN	P52272	HNRNPM HNRPM NAGR1	19,6	2,820E-11
HNRPR_HUMAN	O60506	SYNCRIP HNRPQ NSAP1	21,1	8,970E-11
HNRPU_HUMAN	O43390	HNRNPR HNRPR	5,4	3,150E-07
HP1B3_HUMAN	Q00839	HNRNPU HNRPU SAFA U21.1	12,6	5,930E-07
HSP7C_HUMAN	Q5SSJ5	HP1BP3	3,0	9,450E-08
IF2B1_HUMAN	P11142	HSPA8 HSC70 HSP73 HSPA10	14,7	2,510E-08
IF2B2_HUMAN	Q9NZI8	IGF2BP1 CRDBP VICKZ1 ZBP1	22,6	6,440E-11
IF2B3_HUMAN	Q9Y6M1	IGF2BP2 IMP2 VICKZ2	22,3	4,570E-10
IF2G_HUMAN	O00425	IGF2BP3 IMP3 KOC1 VICKZ3	5,8	2,810E-06
IF2P_HUMAN	P41091	EIF2S3 EIF2G	7,2	2,110E-05
IF4A1_HUMAN	O60841	EIF5B IF2 KIAA0741	7,1	7,890E-08

IF5A1_HUMAN	P60842	EIF4A1 DDX2A EIF4A	18,9	1,500E-08
IF6_HUMAN	P63241	EIF5A	24,7	9,820E-09
IFIT5_HUMAN	P56537	EIF6 EIF3A ITGB4BP OK/SW-cl.27	12,7	2,490E-07
IFRD1_HUMAN	Q13325	IFIT5 ISG58 RI58	13,0	8,150E-09
ILF2_HUMAN	O00458	IFRD1	20,2	1,310E-10
ILF3_HUMAN	Q12905	ILF2 NF45 PRO3063	17,2	2,990E-11
IMA1_HUMAN	Q12906	ILF3 DRBF MPHOSPH4 NF90	16,5	1,790E-07
IQGA1_HUMAN	P52292	KPNA2 RCH1 SRP1	7,6	3,040E-07
K0020_HUMAN	P46940	IQGAP1 KIAA0051	12,0	3,070E-08
K1199_HUMAN	Q15397	KIAA0020 XTP5	10,7	2,830E-10
KRI1_HUMAN	Q8N9T8	KRI1	3,6	5,330E-05
LA_HUMAN	P83111	LACTB MRPL56 UNQ843/PRO1781	27,9	1,870E-07
LACTB_HUMAN	Q92615	LARP4B KIAA0217 LARP5	7,7	3,330E-07
LAR4B_HUMAN	Q6PKG0	LARP1 KIAA0731 LARP	7,6	6,098E-03
LARP1_HUMAN	Q71RC2	LARP4 PP13296	13,6	9,970E-08
LARP4_HUMAN	Q9Y4W2	LAS1L MSTP060	28,0	1,250E-06
LAS1L_HUMAN	P05455	SSB	3,7	2,919E-04
LOXL2_HUMAN	Q9Y4K0	LOXL2	4,6	5,412E-04
LRC59_HUMAN	Q96AG4	LRRC59 PRO1855	12,8	3,300E-09
LRC8A_HUMAN	Q8IWT6	LRRC8A KIAA1437 LRRC8 SWELL1 UNQ221/PRO247	4,1	1,074E-03
LSG1_HUMAN	Q9H089	LSG1	9,3	8,250E-08
LYAR_HUMAN	Q9NX58	LYAR PNAS-5	9,1	4,960E-05
LYRIC_HUMAN	Q86UE4	MTDH AEG1 LYRIC	11,7	2,730E-08
MA2C1_HUMAN	Q9NTJ4	MAN2C1 MANA MANA1	8,5	2,180E-10
MA7D1_HUMAN	Q3KQU3	MAP7D1 KIAA1187 PARCC1 RPRC1 PP2464	8,5	3,610E-05
MAP1A_HUMAN	P78559	MAP1A MAP1L	12,5	1,210E-07
MATR3_HUMAN	P43243	MATR3 KIAA0723	10,2	4,520E-11
MBB1A_HUMAN	Q9BQG0	MYBBP1A P160	15,9	5,340E-10
MICA1_HUMAN	Q8TDZ2	MICAL1 MICAL NICAL	5,6	5,506E-04
MK67I_HUMAN	Q9BYG3	NIFK MKI67IP NOPP34	10,5	1,410E-07
MOV10_HUMAN	Q9HCE1	MOV10 KIAA1631	13,1	1,610E-06
MRCKA_HUMAN	Q5VT25	CDC42BPA KIAA0451	9,7	3,470E-06
MRT4_HUMAN	Q9UKD2	MRTO4 C1orf33 MRT4	20,0	1,840E-08
MYO1B_HUMAN	O43795	MYO1B	4,0	2,090E-05
MYO1C_HUMAN	O00159	MYO1C	6,8	6,440E-11
MYO1D_HUMAN	O94832	MYO1D KIAA0727	12,6	3,150E-11
MYO5A_HUMAN	Q9Y4I1	MYO5A MYH12	9,0	5,450E-06
NACA_HUMAN	Q13765	NACA HSD48	14,6	8,900E-09
NAT10_HUMAN	Q9H0A0	NAT10 ALP KIAA1709	17,2	1,190E-09
NCBP1_HUMAN	Q09161	NCBP1 CBP80 NCBP	10,1	9,670E-05
NEMF_HUMAN	O60524	NEMF SDCCAG1	15,2	3,180E-07
NH2L1_HUMAN	P55769	NHP2L1	29,6	7,930E-09
NHP2_HUMAN	Q9NX24	NHP2 NOLA2 HSPC286	14,4	9,450E-08
NMD3_HUMAN	Q96D46	NMD3 CGI-07	10,9	2,805E-04
NOA1_HUMAN	Q8NC60	NOA1 C4orf14	8,9	6,621E-04
NOG1_HUMAN	Q9BZE4	GTPBP4 CRFG NOG1	18,2	3,950E-07

NOG2_HUMAN	Q13823	GNL2 NGP1	11,6	1,110E-06
NOL6_HUMAN	Q9H6R4	NOL6	10,0	5,250E-06
NONO_HUMAN	Q15233	NONO NRB54	7,9	1,220E-07
NOP10_HUMAN	Q9NPE3	NOP10 NOLA3	26,3	1,880E-06
NOP16_HUMAN	Q9Y3C1	NOP16 CGI-117 HSPC111	26,0	2,730E-08
NOP2_HUMAN	P46087	NOP2 NOL1	15,3	2,880E-11
NOP56_HUMAN	O00567	NOP56 NOL5A	18,2	1,160E-08
NOP58_HUMAN	Q9Y2X3	NOP58 NOL5 NOP5 HSPC120	7,5	4,230E-07
NP1L1_HUMAN	P55209	NAP1L1 NRP	11,7	2,050E-08
NP1L4_HUMAN	Q99733	NAP1L4 NAP2	11,1	7,250E-05
NPM_HUMAN	P06748	NPM1 NPM	22,6	3,410E-10
NSUN2_HUMAN	Q08J23	NSUN2 SAKI TRM4	11,9	4,570E-10
NUCL_HUMAN	P19338	NCL	12,7	3,840E-06
NXF1_HUMAN	Q9UBU9	NXF1 TAP	5,1	2,684E-03
OLA1_HUMAN	Q9NTK5	OLA1 GTPBP9 PRO2455 PTD004	14,3	9,950E-06
P4HA1_HUMAN	P13674	P4HA1 P4HA	4,5	2,180E-08
P4HA2_HUMAN	O15460	P4HA2 UNQ290/PRO330	6,0	4,750E-10
PA2G4_HUMAN	Q9UQ80	PA2G4 EBP1	13,8	2,350E-06
PAB4L_HUMAN	P0CB38	PABPC4L	27,0	4,800E-10
PABP1_HUMAN	P11940	PABPC1 PAB1 PABP1 PABPC2	17,6	1,340E-07
PABP2_HUMAN	Q86U42	PABPN1 PAB2 PABP2	12,1	2,350E-06
PABP3_HUMAN	Q9H361	PABPC3 PABP3 PABPL3	32,4	1,880E-09
PABP4_HUMAN	Q13310	PABPC4 APP1 PABP4	22,0	2,180E-10
PAIRB_HUMAN	Q8NC51	SERBP1 PAIRBP1 CGI-55	19,8	1,060E-06
PCBP1_HUMAN	Q15365	PCBP1	8,2	1,640E-08
PCBP2_HUMAN	Q15366	PCBP2	14,2	2,740E-09
PDCD4_HUMAN	Q53EL6	PDCD4 H731	15,3	6,770E-09
PDIA1_HUMAN	P07237	P4HB ERBA2L PDI PDIA1 PO4DB	4,9	3,560E-08
PESC_HUMAN	O00541	PES1	7,3	5,730E-08
PLEC_HUMAN	Q15149	PLEC PLEC1	17,2	1,490E-06
PLOD1_HUMAN	Q02809	PLOD1 LLH PLOD	8,9	1,840E-08
PLOD3_HUMAN	O60568	PLOD3	4,4	2,510E-06
PLPL6_HUMAN	Q8IY17	PNPLA6 NTE	5,5	3,900E-05
POP1_HUMAN	Q99575	POP1 KIAA0061	6,5	1,030E-05
PRC2C_HUMAN	Q9Y520	PRRC2C BAT2D1 BAT2L2 KIAA1096 XTP2	7,7	2,510E-06
PRDBP_HUMAN	Q969G5	PRKCDBP SRBC	12,3	1,370E-06
PRKRA_HUMAN	O75569	PRKRA PACT RAX HSD-14 HSD14	15,9	1,500E-07
PRP19_HUMAN	Q9UMS4	PRPF19 NMP200 PRP19 SNEV	10,6	2,750E-07
PRP4_HUMAN	O43172	PRPF4 PRP4	13,3	3,910E-07
PRP8_HUMAN	Q6P2Q9	PRPF8 PRPC8	4,2	1,578E-04
PTBP1_HUMAN	P26599	PTBP1 PTB	15,1	4,520E-11
PTRF_HUMAN	Q6NZI2	PTRF FKSG13	18,0	1,140E-08
PURA_HUMAN	Q00577	PURA PUR1	34,2	5,920E-10
PURB_HUMAN	Q96QR8	PURB	26,7	5,340E-10
PWP1_HUMAN	Q13610	PWP1	12,0	5,490E-09
RALY_HUMAN	Q9UKM9	RALY HNRPCL2 P542	13,6	4,560E-07

RBM28_HUMAN	Q9NW13	RBM28	9,0	4,340E-05
RBM3_HUMAN	P42696	RBM34 KIAA0117	11,8	2,250E-09
RBM34_HUMAN	Q14498	RBM39 HCC1 RNPC2	11,0	5,550E-06
RBM39_HUMAN	P98179	RBM3 RNPL	12,7	3,890E-09
RBM4_HUMAN	Q9BQ04	RBM4B RBM30	16,1	4,120E-07
RBM4B_HUMAN	Q9BWF3	RBM4 RBM4A	46,9	4,720E-06
RBM8A_HUMAN	Q9Y5S9	RBM8A RBM8 HSPC114 MDS014	14,5	6,620E-08
RBMS1_HUMAN	P29558	RBMS1 C2orf12 MSSP MSSP1 SCR2	13,5	5,690E-08
RBMS2_HUMAN	Q15434	RBMS2 SCR3	11,2	1,173E-04
RBMS3_HUMAN	Q6XE24	RBMS3	11,9	7,840E-06
RBMX_HUMAN	P38159	RBMX HNRPG RBMXP1	8,1	6,770E-09
RBP56_HUMAN	Q92804	TAF15 RBP56 TAF2N	3,5	1,270E-07
RED1_HUMAN	P78563	ADARB1 ADAR2 DRADA2 RED1	7,3	2,110E-07
RENT1_HUMAN	Q92900	UPF1 KIAA0221 RENT1	7,6	1,120E-06
RL10_HUMAN	P62906	RPL10A NEDD6	42,3	5,560E-08
RL10A_HUMAN	P27635	RPL10 DXS648E QM	31,7	8,700E-08
RL11_HUMAN	P62913	RPL11	23,2	5,270E-07
RL12_HUMAN	P30050	RPL12	48,4	2,550E-11
RL13_HUMAN	P40429	RPL13A	32,1	3,570E-08
RL13A_HUMAN	P26373	RPL13 BBC1 OK/SW-cl.46	27,5	4,310E-08
RL14_HUMAN	P50914	RPL14	34,2	1,290E-08
RL15_HUMAN	P61313	RPL15 EC45 TCBAP0781	25,1	8,490E-09
RL17_HUMAN	P18621	RPL17	33,2	1,260E-08
RL18_HUMAN	Q02543	RPL18A	34,9	4,180E-08
RL18A_HUMAN	Q07020	RPL18	38,4	1,020E-08
RL19_HUMAN	P84098	RPL19	32,2	8,200E-09
RL1D1_HUMAN	O76021	RSL1D1 CATX11 CSIG PBK1 L12	38,6	4,150E-09
RL21_HUMAN	P46778	RPL21	36,9	5,360E-09
RL22_HUMAN	Q6P5R6	RPL22L1	42,7	9,970E-13
RL22L_HUMAN	P35268	RPL22	48,9	8,970E-11
RL23_HUMAN	P62750	RPL23A	39,4	2,820E-11
RL23A_HUMAN	P62829	RPL23	31,5	1,200E-07
RL24_HUMAN	P83731	RPL24	17,1	3,410E-10
RL26_HUMAN	Q9UNX3	RPL26L1 RPL26P1	31,5	8,240E-08
RL26L_HUMAN	P61254	RPL26	40,6	8,100E-11
RL27_HUMAN	P46776	RPL27A	56,1	8,920E-11
RL27A_HUMAN	P61353	RPL27	65,0	1,900E-11
RL28_HUMAN	P46779	RPL28	61,9	2,690E-11
RL29_HUMAN	P47914	RPL29	27,8	7,840E-08
RL3_HUMAN	P62888	RPL30	37,5	1,740E-09
RL30_HUMAN	P62899	RPL31	71,8	1,250E-10
RL31_HUMAN	P62910	RPL32 PP9932	40,8	6,440E-11
RL32_HUMAN	P49207	RPL34	32,3	1,290E-11
RL34_HUMAN	P18077	RPL35A GIG33	49,0	1,690E-10
RL35_HUMAN	P42766	RPL35	44,6	1,570E-09
RL35A_HUMAN	P83881	RPL36A RPL44 GIG15 MIG6	52,4	2,040E-11

RL36_HUMAN	Q9Y3U8	RPL36	43,2	4,520E-11
RL36A_HUMAN	P61513	RPL37A	47,8	1,840E-10
RL37A_HUMAN	P63173	RPL38	53,2	2,900E-10
RL38_HUMAN	P39023	RPL3 OK/SW-cl.32	127,7	1,230E-10
RL4_HUMAN	P62987	UBA52 UBCEP2	38,8	5,830E-08
RL40_HUMAN	P36578	RPL4 RPL1	18,5	2,151E-03
RL5_HUMAN	P46777	RPL5 MSTP030	42,8	1,440E-09
RL6_HUMAN	Q02878	RPL6 TXREB1	41,2	1,330E-09
RL7_HUMAN	P62424	RPL7A SURF-3 SURF3	34,5	1,780E-08
RL7A_HUMAN	Q6DKI1	RPL7L1	29,6	1,670E-05
RL7L_HUMAN	P18124	RPL7	49,3	3,530E-06
RL8_HUMAN	P62917	RPL8	19,7	1,980E-05
RL9_HUMAN	P32969	RPL9 OK/SW-cl.103; RPL9P7; RPL9P8; RPL9P9	38,1	2,290E-08
RLA0_HUMAN	P05388	RPLP0	10,8	1,440E-05
RLA1_HUMAN	P05386	RPLP1 RRP1	30,7	2,090E-09
RLA2_HUMAN	P05387	RPLP2 D11S2243E RPP2	57,1	5,510E-13
RM01_HUMAN	Q9BYD6	MRPL1 BM-022	7,1	4,604E-04
RM23_HUMAN	Q16540	MRPL23 L23MRP RPL23L	12,6	2,750E-07
RN213_HUMAN	Q63HN8	RNF213 ALO17 C17orf27 KIAA1554 KIAA1618 MYSTR	7,0	1,385E-04
RO60_HUMAN	P10155	TROVE2 RO60 SSA2	11,4	2,820E-05
ROA0_HUMAN	Q13151	HNRNPA0 HNRPA0	11,6	1,560E-07
ROA1_HUMAN	P09651	HNRNPA1 HNRPA1	18,2	2,710E-10
ROA2_HUMAN	P22626	HNRNPA2B1 HNRPA2B1	14,0	4,130E-10
ROA3_HUMAN	P51991	HNRNPA3 HNRPA3	10,4	5,760E-08
ROAA_HUMAN	Q99729	HNRNPAB ABBP1 HNRPAB	17,4	5,920E-10
RPF2_HUMAN	Q9H7B2	RPF2 BXDC1	19,0	6,320E-09
RPN1_HUMAN	P04843	RPN1	7,5	2,280E-07
RPN2_HUMAN	P04844	RPN2	5,2	1,450E-07
RRBP1_HUMAN	Q9P2E9	RRBP1 KIAA1398	3,4	5,790E-06
RRP1_HUMAN	Q5JTH9	RRP12 KIAA0690	23,5	2,165E-04
RRP12_HUMAN	Q14684	RRP1B KIAA0179	7,6	4,490E-08
RRP1B_HUMAN	P56182	RRP1 D21S2056E NNP1 NOP52 RRP1A	12,4	2,650E-06
RRP5_HUMAN	Q14690	PDCD11 KIAA0185	4,3	3,554E-04
RRP8_HUMAN	O43159	RRP8 KIAA0409 NML hucep-1	13,5	1,210E-07
RRS1_HUMAN	Q15050	RRS1 KIAA0112 RRR	11,7	1,260E-07
RS10_HUMAN	P46783	RPS10	46,1	6,920E-13
RS11_HUMAN	P62280	RPS11	48,3	5,950E-10
RS12_HUMAN	P25398	RPS12	43,3	5,510E-13
RS13_HUMAN	P62277	RPS13	59,8	8,370E-13
RS14_HUMAN	P62263	RPS14 PRO2640	55,7	5,510E-13
RS15_HUMAN	P62244	RPS15A OK/SW-cl.82	21,4	1,250E-10
RS15A_HUMAN	P62841	RPS15 RIG	40,2	8,920E-11
RS16_HUMAN	P62249	RPS16	55,9	3,150E-11
RS17L_HUMAN	P0CW22	RPS17L	39,3	3,630E-11
RS18_HUMAN	P62269	RPS18 D6S218E	55,7	6,440E-11
RS19_HUMAN	P39019	RPS19	63,6	3,140E-11

RS2_HUMAN	P60866	RPS20	8,8	2,310E-06
RS20_HUMAN	P63220	RPS21	55,0	1,980E-10
RS21_HUMAN	P62266	RPS23	48,3	1,220E-10
RS23_HUMAN	P62847	RPS24	37,5	4,020E-10
RS24_HUMAN	P62851	RPS25	39,6	2,540E-10
RS25_HUMAN	P62854	RPS26	47,9	6,440E-11
RS26_HUMAN	P62979	RPS27A UBA80 UBCEP1	48,3	4,520E-11
RS27_HUMAN	Q71UM5	RPS27L	35,0	2,350E-08
RS27A_HUMAN	P42677	RPS27 MPS1	52,6	2,820E-11
RS27L_HUMAN	P62857	RPS28	32,8	1,090E-08
RS28_HUMAN	P62273	RPS29	56,6	4,510E-10
RS29_HUMAN	P15880	RPS2 RPS4	43,4	5,420E-11
RS3_HUMAN	P62861	FAU	9,0	4,850E-05
RS30_HUMAN	P61247	RPS3A FTE1 MFTL	39,7	4,580E-09
RS3A_HUMAN	P23396	RPS3 OK/SW-cl.26	5,8	7,770E-06
RS4X_HUMAN	P62701	RPS4X CCG2 RPS4 SCAR	30,3	1,470E-07
RS5_HUMAN	P46782	RPS5	31,6	2,460E-08
RS6_HUMAN	P62753	RPS6 OK/SW-cl.2	35,5	2,600E-10
RS7_HUMAN	P62081	RPS7	34,1	3,070E-08
RS8_HUMAN	P62241	RPS8 OK/SW-cl.83	29,6	1,920E-08
RS9_HUMAN	P46781	RPS9	36,9	3,080E-08
RSSA_HUMAN	P08865	RPSA LAMBR LAMR1	17,5	9,220E-06
RT05_HUMAN	P82675	MRPS5	5,4	1,125E-02
RT18B_HUMAN	Q9Y676	MRPS18B C6orf14 HSPC183 PTD017	17,0	8,940E-05
RT22_HUMAN	P82650	MRPS22 C3orf5 RPMS22 GK002	4,0	6,482E-04
RT23_HUMAN	Q9Y3D9	MRPS23 CGI-138 HSPC329	7,5	1,122E-03
RT27_HUMAN	Q92552	MRPS27 KIAA0264	21,1	1,117E-02
RT28_HUMAN	Q9Y2Q9	MRPS28 MRPS35 HSPC007	14,6	1,563E-03
RT34_HUMAN	P82930	MRPS34	9,5	1,104E-04
RTCB_HUMAN	Q9Y3I0	RTCB C22orf28 HSPC117	6,0	2,820E-11
RU17_HUMAN	P08621	SNRNP70 RNPU1Z RPU1 SNRP70 U1AP1	13,0	4,390E-08
RUVB1_HUMAN	Q9Y265	RUVBL1 INO80H NMP238 TIP49 TIP49A	7,5	1,190E-06
RUVB2_HUMAN	Q9Y230	RUVBL2 INO80J TIP48 TIP49B CGI-46	6,0	1,340E-06
RUXE_HUMAN	P62304	SNRPE	15,1	6,430E-09
RUXF_HUMAN	P62306	SNRPF PBSCF	15,0	1,250E-08
S61A1_HUMAN	P61619	SEC61A1 SEC61A	18,9	2,290E-08
SAFB1_HUMAN	Q15424	SAFB HAP HET SAFB1	3,9	1,850E-06
SART3_HUMAN	Q15020	SART3 KIAA0156 TIP110	6,2	5,215E-04
SC61B_HUMAN	P60468	SEC61B	36,4	8,060E-09
SDA1_HUMAN	Q9NVU7	SDAD1 NUC130	16,2	5,250E-06
SF3B1_HUMAN	O75533	SF3B1 SAP155	9,2	2,986E-04
SF3B3_HUMAN	Q15393	SF3B3 KIAA0017 SAP130	4,9	3,280E-06
SFPQ_HUMAN	P23246	SFPQ PSF	11,2	5,950E-10
SK2L2_HUMAN	P42285	SKIV2L2 KIAA0052 Mtr4	14,4	7,920E-08
SKIV2_HUMAN	Q15477	SKIV2L DDX13 SKI2W SKIV2 W	9,9	5,900E-06
SMBP2_HUMAN	P38935	IGHMBP2 SMBP2 SMUBP2	7,1	5,800E-04

SMD1_HUMAN	P62314	SNRPD1	15,2	8,060E-09
SMD2_HUMAN	P62316	SNRPD2 SNRPD1	8,8	3,244E-03
SMD3_HUMAN	P62318	SNRPD3	15,5	8,920E-11
SND1_HUMAN	Q7KZF4	SND1 TDRD11	22,3	6,050E-11
SNRPA_HUMAN	P09012	SNRPA	13,0	1,450E-08
SPAS2_HUMAN	Q86XZ4	SPATS2 SCR59 SPATA10 Nbla00526	10,6	1,120E-05
SPB1_HUMAN	Q8IY81	FTSJ3 SB92	10,2	1,880E-09
SPS2L_HUMAN	Q9NUQ6	SPATS2L DNAPTP6 SP1224	18,3	1,220E-10
SRP09_HUMAN	P49458	SRP9	8,8	3,500E-07
SRP14_HUMAN	P37108	SRP14	43,2	1,020E-08
SRP54_HUMAN	P61011	SRP54	6,4	1,860E-05
SRP68_HUMAN	Q9UHB9	SRP68	12,2	3,650E-07
SRP72_HUMAN	O76094	SRP72	5,0	4,437E-04
SRPK1_HUMAN	Q96SB4	SRPK1	14,2	3,168E-02
SRPK2_HUMAN	P78362	SRPK2	15,6	6,750E-08
SRSF1_HUMAN	Q07955	SRSF1 ASF SF2 SF2P33 SFRS1 OK/SW-cl.3	14,3	6,000E-09
SRSF3_HUMAN	P84103	SRSF3 SFRS3 SRP20	22,8	1,430E-09
SRSF4_HUMAN	Q08170	SRSF4 SFRS4 SRP75	12,6	2,340E-05
SRSF5_HUMAN	Q13243	SRSF5 HRS SFRS5 SRP40	19,9	3,220E-07
SRSF6_HUMAN	Q13247	SRSF6 SFRS6 SRP55	20,2	7,530E-09
SRSF7_HUMAN	Q16629	SRSF7 SFRS7	8,9	3,908E-04
SSF1_HUMAN	Q9NQ55	PPAN BXDC3 SSF1	11,6	5,050E-07
STAU2_HUMAN	Q9NUL3	STAU2	6,6	2,230E-05
SULF1_HUMAN	Q8IWU6	SULF1 KIAA1077	13,7	1,390E-08
SYDC_HUMAN	P14868	DARS PIG40	3,9	5,940E-06
SYEP_HUMAN	P07814	EPRS GLNS PARS QARS QPRS PIG32	4,9	6,430E-09
SYFA_HUMAN	Q9Y285	FARSA FARS FARSL FARSLA	12,6	4,860E-08
SYFB_HUMAN	Q9NSD9	FARSB FARSLB FRSB HSPC173	13,7	2,770E-09
SYIC_HUMAN	P41252	IARS	4,5	8,170E-09
SYK_HUMAN	Q15046	KARS KIAA0070	6,6	9,680E-06
SYLC_HUMAN	Q9P2J5	LARS KIAA1352	3,5	5,249E-03
SYMC_HUMAN	P56192	MARS	3,6	2,000E-05
SYNM_HUMAN	Q96I59	NARS2	12,4	1,780E-06
SYQ_HUMAN	P47897	QARS	4,2	1,410E-07
SYRC_HUMAN	P54136	RARS	4,9	2,490E-07
SYYC_HUMAN	P54577	YARS	8,7	1,660E-06
TADBP_HUMAN	Q13148	TARDBP TDP43	15,6	2,720E-05
TBL2_HUMAN	Q9Y4P3	TBL2 WBSCR13 UNQ563/PRO1125	15,4	1,560E-08
TF3C1_HUMAN	Q12789	GTF3C1	4,0	1,666E-02
THOC4_HUMAN	Q86V81	ALYREF ALY BEF THOC4	12,6	2,090E-09
TOP1_HUMAN	P11387	TOP1	15,1	1,020E-06
TR150_HUMAN	Q9Y2W1	THRAP3 TRAP150	3,2	9,509E-03
TRA2B_HUMAN	P62995	TRA2B SFRS10	8,9	1,058E-04
TRI56_HUMAN	Q9BRZ2	TRIM56 RNF109	8,8	1,080E-06
TRIPC_HUMAN	Q14669	TRIP12 KIAA0045 ULF	9,8	1,340E-07
TRM1L_HUMAN	Q7Z2T5	TRMT1L C1orf25 TRM1L MSTP070	11,2	2,250E-09

TSP1_HUMAN	P07996	THBS1 TSP TSP1	5,5	2,670E-07
TTC37_HUMAN	Q6PGP7	TTC37 KIAA0372	16,3	5,920E-10
U2AF2_HUMAN	P26368	U2AF2 U2AF65	7,0	1,780E-08
U3IP2_HUMAN	O43818	RRP9 RNU3IP2 U355K	14,0	6,890E-07
U520_HUMAN	O75643	SNRNP200 ASCC3L1 HELIC2 KIAA0788	6,4	1,350E-06
U5S1_HUMAN	Q15029	EFTUD2 KIAA0031 SNRP116	7,5	1,450E-07
VIGLN_HUMAN	Q00341	HDLBP HBP VGL	6,1	1,930E-06
WDR36_HUMAN	Q8NI36	WDR36	10,1	3,908E-04
WIBG_HUMAN	Q9BRP8	WIBG PYM	14,0	1,400E-06
XRCC5_HUMAN	P13010	XRCC5 G22P2	4,0	6,920E-05
XRCC6_HUMAN	P12956	XRCC6 G22P1	6,3	4,690E-06
XRN2_HUMAN	Q9H0D6	XRN2	4,4	2,106E-03
YBOX1_HUMAN	P67809	YBX1 NSEP1 YB1	18,1	1,990E-06
YBOX3_HUMAN	P16989	YBX3 CSDA DBPA	19,7	1,680E-06
YTDC2_HUMAN	Q9H6S0	YTHDC2	8,9	5,600E-06
ZCCHV_HUMAN	Q7Z2W4	ZC3HAV1 ZC3HDC2 PRO1677	12,2	7,810E-08
ZFP91_HUMAN	Q96JP5	ZFP91 ZNF757 FKSG11	23,8	3,970E-08
ZFR_HUMAN	Q96KR1	ZFR	14,5	4,740E-07
ZN326_HUMAN	Q5BKZ1	ZNF326 ZIRD	14,8	3,640E-07
ZN622_HUMAN	Q969S3	ZNF622 ZPR9	16,7	2,700E-10

Supplementary Table 1. Proteins enriched in Chemical Proteomics analysis

From pulldown experiments with active and inactive compound, 430 proteins were identified showing ≥1.5-fold enrichment for the Active compound (adjusted $p \leq 0.05$). Using the GO_SLIM collection of gene ontology annotations (http://ceur-ws.org/Vol-1546/paper_44.pdf), enrichment for 8 pathway categories was found based on Fisher's exact test (cutoff for $p<0.001$), illustrated by negative logarithm of the enrichment p value on the x axis of Figure 1E. Reasoning that proteins involved in the translational machinery would be associated through their interactions with RNA, a second list of 339 proteins was created by manually removing ribosomal proteins form the 430 proteins. Repeating the enrichment analysis, smaller enrichment p values were obtained with the exception of the "RNA splicing" category (y axis in Figure 1E), which scored substantially better. We conclude that this category is the strongest hit independent of the (inevitable) presence of ribosomal proteins in our data set.

ΔPSI	SMN-C3	NVS-SM1
ABCB8	0,398	0,670
ANKRD36	0,035	0,578
APLP2	0,270	0,466
ARHGAP12	0,016	0,438
ARMCX6	0,010	0,499
ASAP1	0,355	0,733
ATG5	0,027	0,446
AXIN1	0,069	0,665
BIRC6	0,039	0,563
C1orf86	0,043	0,572
CDC42BPA	0,146	0,560
CLTA	0,239	0,473
DYRK1A	0,007	0,414
ERGIC3	0,035	0,439
FBXL6	0,461	0,037
FOXM1	0,417	0,470
GGCT	0,455	0,362
KAT6B	0,047	0,707
KDM6A	0,082	0,404
KIF3A	0,219	0,681
KMT2D	0,048	0,647
LARP7	0,404	0,864
LYRM1	0,139	0,686
MADD	0,073	0,797
MAN2C1	0,461	0,033
MRPL55	0,448	0,013
MYCBP2	0,111	0,511
MYO9B	0,506	0,031
PNISR	0,028	0,765
RAP1A	0,246	0,504
RAPGEF1	0,552	0,402
SENP6	0,364	0,567
SH3YL1	0,131	0,566
SLC25A17	0,644	0,481
SMN2	0,429	0,537
SREK1	0,021	0,466
STRN3	0,556	0,860
TAF2	0,217	0,710
TMEM134	0,444	0,009
VPS29	0,422	0,671
ZFAND1	0,024	0,408
ZNF431	0,111	0,468

Supplementary Table 2. Splicing changes from RNAseq study

Data express changes in SMN2 FL/Δ7 splicing ratio upon compound treatment as delta % spliced in (ΔPSI), shown in Fig. 3B. Data were averaged from five independent samples.

		abs(logFC)	
Name	Description	SMN-C3	NVS-SM1
100507053	-	1,316	1,967
100507424	-	0,668	1,451
101928588	-	0,595	1,746
101928711	-	0,59	1,828
100289187	-	0,146	1,511
653513	-	0,134	1,220
100288152	-	0,11	1,179
25845	-	0,049	1,142
4363	ABCC1	0,053	0,966
59	ACTA2	0,292	1,141
161823	ADAL	0,238	1,302
8038	ADAM12	0,002	1,868
9510	ADAMTS1	0,04	1,137
11096	ADAMTS5	0,072	1,380
118	ADD1	0,027	0,989
57211	ADGRG6	0,052	1,128
137872	ADHFE1	0,245	1,491
55750	AGK	0,182	1,159
8540	AGPS	0,33	1,842
651746	ANKRD33B	0,017	1,145
311	ANXA11	0,045	1,142
309	ANXA6	0,068	1,224
84159	ARID5B	0,082	0,906
132946	ARL9	0,962	1,627
51566	ARMCX3	0,516	1,252
50807	ASAP1	0,156	1,729
41	ASIC1	0,246	2,102
54454	ATAD2B	0,558	0,697
594	BCKDHB	0,095	0,976
440603	BCL2L15	0,204	4,557
618	BCYRN1	1,002	1,991
7832	BTG2	0,121	0,938
64115	C10ORF54	0,147	1,068
85016	C11ORF70	0,084	1,177
51501	C11ORF73	0,958	0,945
115749	C12ORF56	0,125	1,522
126526	C19ORF47	0,353	1,643
54969	C4ORF27	0,714	1,487
782	CACNB1	0,429	2,565
23705	CADM1	0,235	1,053
23066	CAND2	1,038	1,721
22794	CASC3	0,332	0,563
899	CCNF	0,014	0,864
83879	CDCA7	0,561	1,734

54901	CDKAL1	0,274	0,977
57214	CEMIP	0,175	2,044
9859	CEP170	0,139	1,833
3075	CFH	0,158	1,071
57396	CLK4	0,398	0,650
8418	CMAHP	0,523	1,458
124817	CNTD1	0,096	2,575
1301	COL11A1	0,212	1,451
1303	COL12A1	0,069	1,698
1289	COL5A1	0,046	0,953
50509	COL5A3	0,023	0,989
1295	COL8A1	0,044	1,204
81035	COLEC12	0,138	1,449
1311	COMP	0,213	1,519
51200	CPA4	0,355	1,342
10404	CPQ	0,401	1,166
83716	CRISPLD2	0,101	1,103
9244	CRLF1	0,054	0,932
51084	CRYL1	0,353	1,953
1503	CTPS1	0,364	0,441
1523	CUX1	0,046	0,902
80777	CYB5B	0,004	1,485
51700	CYB5R2	0,227	1,829
114757	CYGB	0,207	1,236
1545	CYP1B1	0,296	2,496
1634	DCN	0,131	0,924
23142	DCUN1D4	0,367	0,356
115265	DDIT4L	0,18	1,067
11325	DDX42	0,117	1,131
79009	DDX50	0,194	0,979
8560	DEGS1	0,022	1,017
57706	DENND1A	1,284	1,426
23258	DENND5A	0,74	2,090
494513	DFNB59	0,172	1,198
1606	DGKA	0,268	0,938
1719	DHFR	0,436	2,079
81624	DIAPH3	0,862	3,346
9077	DIRAS3	0,044	1,012
115752	DIS3L	0,059	0,910
9231	DLG5	0,051	1,276
51277	DNAJC27	0,701	1,396
1793	DOCK1	0,438	0,660
139818	DOCK11	0,031	1,704
1780	DYNC1I1	0,078	1,720
199221	DZIP1L	0,089	1,266
1879	EBF1	0,038	1,119

2202	EFEMP1	0,073	1,433
8891	EIF2B3	0,602	2,126
2006	ELN	0,026	1,077
26610	ELP4	0,076	2,330
196047	EMX2OS	0,036	1,161
5167	ENPP1	0,03	0,918
2034	EPAS1	0,051	0,984
1161	ERCC8	0,202	0,968
11082	ESM1	0,438	2,206
132884	EVC2	0,176	1,180
2149	F2R	0,217	1,562
51313	FAM198B	0,215	1,617
115572	FAM46B	0,177	1,079
2191	FAP	0,273	1,139
10160	FARP1	0,063	1,349
2199	FBLN2	0,121	1,460
2201	FBN2	0,119	1,620
26267	FBXO10	0,513	0,524
26268	FBXO9	0,27	2,108
2241	FER	0,406	1,603
2263	FGFR2	0,11	1,396
8061	FOSL1	0,371	0,342
80144	FRAS1	0,025	1,837
79690	GAL3ST4	0,176	0,927
2581	GALC	1,559	1,312
2627	GATA6	0,203	1,214
26301	GBGT1	0,101	1,159
2650	GCNT1	0,023	1,165
2776	GNAQ	0,085	1,724
2804	GOLGB1	0,218	0,917
51704	GPRC5B	0,269	1,288
283464	GXYLT1	0,093	1,372
3038	HAS3	0,281	3,333
84868	HAVCR2	0,187	5,032
10014	HDAC5	0,01	1,476
9843	HEPH	0,117	0,932
6596	HLTF	0,898	1,082
3162	HMOX1	0,108	2,069
84376	HOOK3	0,06	1,032
51144	HSD17B12	0,569	1,981
3305	HSPA1L	0,163	2,486
10553	HTATIP2	0,073	0,944
3064	HTT	0,551	1,288
3482	IGF2R	0,098	1,517
3486	IGFBP3	0,082	1,012
9118	INA	0,005	1,249

27152	INTU	0,334	1,084
84223	IQCG	0,013	1,024
22801	ITGA11	0,144	1,427
3706	ITPKA	0,051	1,555
7403	KDM6A	0,23	1,335
2531	KDSR	0,042	1,105
57604	KIAA1456	0,124	1,168
57608	KIAA1462	0,052	1,050
57650	KIAA1524	0,477	2,072
80856	KIAA1715	0,378	1,161
3815	KIT	0,214	1,801
3855	KRT7	0,086	1,099
81851	KRTAP1-1	0,072	0,975
83895	KRTAP1-5	0,062	1,222
83746	L3MBTL2	0,038	0,943
55366	LGR4	0,203	0,938
79940	LINC00472	0,325	1,415
100505566	LINC00578	0,028	1,221
646324	LINC00607	0,14	1,198
100652988	LINC00702	0,007	1,342
25802	LMOD1	0,213	1,192
987	LRBA	0,016	0,990
4038	LRP4	0,07	1,439
2615	LRRC32	0,09	1,530
127495	LRRC39	0,908	2,805
4045	LSAMP	0,185	2,154
4060	LUM	0,208	1,287
116372	LYPD1	0,065	0,909
57149	LYRM1	0,015	0,886
9935	MAFB	0,063	1,192
10905	MAN1A2	0,175	1,257
4124	MAN2A1	0,044	0,949
5603	MAPK13	0,018	0,856
5648	MASP1	0,292	1,341
84935	MEDAG	1,097	2,649
1953	MEGF6	0,103	0,996
51072	MEMO1	0,381	1,173
693197	MIR612	0,692	2,380
8028	MLLT10	0,058	0,878
4319	MMP10	0,431	0,871
10893	MMP24	0,107	1,317
64210	MMS19	0,175	1,064
4330	MN1	0,216	1,052
26002	MOXD1	0,126	0,921
10335	MRVI1	0,27	1,184
51001	MTERF3	0,626	0,644

25878	MXRA5	0,126	2,191
4642	MYO1D	0,158	2,088
8883	NAE1	0,047	0,895
162417	NAGS	0,251	1,206
79625	NDNF	0,041	1,154
54492	NEURL1B	0,254	0,965
57486	NLN	0,127	1,591
4854	NOTCH3	0,033	0,960
10886	NPFFR2	0,752	0,717
22854	NTNG1	0,282	1,023
100506658	OCLN	0,033	1,366
64064	OXCT2	0,134	1,230
167153	PAPD4	1,155	1,492
64081	PBLD	0,08	1,158
5108	PCM1	0,142	1,914
5137	PDE1C	0,164	1,145
8654	PDE5A	0,077	1,282
5159	PDGFRB	0,087	1,008
23047	PDS5B	0,065	1,673
23042	PDXDC1	1,673	2,015
375033	PEAR1	0,165	1,144
5184	PEPD	0,207	0,994
26147	PHF19	0,382	0,042
55300	PI4K2B	0,165	1,133
5295	PIK3R1	0,204	0,941
11040	PIM2	0,061	0,971
23760	PITPNB	0,693	2,516
83394	PITPNM3	0,063	1,350
5328	PLAU	0,606	0,645
26499	PLEK2	0,054	0,888
22874	PLEKHA6	0,043	1,425
130271	PLEKHH2	0,135	1,548
10154	PLXNC1	0,214	1,714
5378	PMS1	0,777	1,319
127435	PODN	0,014	1,197
353497	POLN	1,108	0,544
25885	POLR1A	0,004	1,651
10631	POSTN	0,225	0,884
5530	PPP3CA	0,093	1,333
5578	PRKCA	0,021	0,992
5591	PRKDC	0,111	1,726
5592	PRKG1	0,147	1,131
5961	PRPH2	0,241	1,051
100507062	PSMD6-AS2	0,201	1,005
5740	PTGIS	0,085	1,433
5806	PTX3	0,064	1,035

27314	RAB30	0,141	1,066
5917	RARS	0,009	0,908
5932	RBBP8	0,131	1,816
64080	RBKS	0,146	1,186
1104	RCC1	0,329	3,358
5962	RDX	0,11	2,309
64326	RFWD2	0,435	1,943
101929302	RFX3-AS1	1,092	2,386
28984	RGCC	0,304	1,316
51136	RNFT1	0,112	1,127
4919	ROR1	0,121	1,224
201965	RWDD4	0,18	0,946
619383	SCARNA9	1,339	1,209
6341	SCO1	0,137	1,280
26984	SEC22A	0,69	0,833
57619	SHROOM3	0,187	1,055
57181	SLC39A10	0,061	0,930
83959	SLC4A11	0,127	1,634
23657	SLC7A11	0,006	0,908
6550	SLC9A3	0,354	1,042
6586	SLIT3	0,009	1,054
100271836	SMG1P3	0,624	0,790
6525	SMTN	0,274	1,123
64754	SMYD3	0,1	0,961
25992	SNED1	0,022	1,164
100507246	SNHG16	0,435	1,062
57537	SORCS2	0,109	0,949
57213	SPRYD7	0,391	0,849
58472	SQRDL	0,651	0,876
6772	STAT1	0,553	1,162
261729	STEAP2	0,916	2,899
55351	STK32B	0,004	1,001
29888	STRN4	0,014	1,445
412	STS	0,114	1,228
29091	STXBP6	0,06	0,991
23213	SULF1	0,07	1,131
79987	SVEP1	0,157	1,741
9144	SYNGR2	0,08	1,463
11346	SYNPO	0,069	1,105
171024	SYNPO2	0,211	1,849
4070	TACSTD2	0	1,165
29114	TAGLN3	0,253	1,142
79613	TANGO6	0,01	1,059
6894	TARBP1	0,659	1,401
441687	TEX21P	3,517	2,427
7039	TGFA	0,153	0,832

7043	TGFB3	0,148	1,044
7052	TGM2	0,043	0,993
63892	THADA	0,531	1,759
7058	THBS2	0,157	1,364
284114	TMEM102	0,151	1,019
338773	TMEM119	0,197	1,077
100529211	TMEM256-PLSCR3	0,668	1,867
757	TMEM50B	0,104	0,918
3371	TNC	0,092	0,959
388121	TNFAIP8L3	0,092	1,097
8764	TNFRSF14	0,208	1,419
64759	TNS3	0,681	2,764
7148	TNXB	0,141	1,194
401505	TOMM5	0,452	0,389
7187	TRAF3	0,045	0,988
7223	TRPC4	0,207	1,522
128553	TSHZ2	0,028	1,224
90139	TSPAN18	0,266	1,377
81629	TSSK3	0,045	1,000
10628	TXNIP	0,21	1,275
219699	UNC5B	0,183	0,926
7405	UVRAG	0,123	0,997
100507347	VIM-AS1	0,228	1,463
27072	VPS41	0,041	1,441
128434	VSTM2L	0,111	1,863
23078	VWA8	0,032	1,341
29062	WDR91	0,273	0,895
8840	WISP1	0,228	1,007
22803	XRN2	0,376	2,311
150223	YDJC	0,067	0,840
26137	ZBTB20	0,523	0,204
57684	ZBTB26	0,269	1,649
284406	ZFP82	0,224	0,963
7988	ZNF212	0,041	0,892
284695	ZNF326	0,352	0,135
59348	ZNF350	0,178	0,936
7633	ZNF79	0,041	1,075
116412	ZNF837	2,469	3,044

Supplementary Table 3. Transcriptional changes from RNAseq study

Data express changes in transcription upon compound treatment as log2 fold change, shown in Fig. 3C. Data were averaged from five independent samples.

Inhibitor	Concentration
Actinomycin D	1µg/ml
Cordycepin (3-deoxyadenosine)	500nM
α-Amanitin	50µg/ml
Puromycin dihydrochloride	10µg/ml
Pladienolide-B	10µM
Isoginkgetin	50µM

Supplementary Table 4. Concentration of inhibitors used in cell experiments (Fig. 1, Supplementary Fig. 2).

target name	primer/probe	sequence (5' -> 3')
SMN2 (full length)	forward primer (exon 7/8)	GCTCACATTCCTTAAATTAAGGAGAAA
	reverse primer (exon 8)	TCCAGATCTGTCTGATCGTTTCTT
	5'FAM/3'BHQ1-probe (exon 8)	CTGGCATAGAGCAGCACTAAATGACACCAC
SMN2 (delta exon 7)	forward primer (exon 6/8)	TGGCTATCATACTGGCTATTATATGGAA
	reverse primer (exon 8)	TCCAGATCTGTCTGATCGTTTCTT
	5'FAM/3'BHQ1-probe (exon 8)	CTGGCATAGAGCAGCACTAAATGACACCAC
STRN3 (full length)	forward primer (exon 8/9)	GGAAGAAAGGGGTGAAGAGG
	reverse primer (exon 9)	TGATTCCTGAAGGGATGTGG
	5'FAM/3'BHQ1-UPL-probe (exon 9)	CTGGGAGA
STRN3 (delta exon 8/9)	forward primer (exon 7/10)	CAGAATGGGCTGAACCAATAA
	reverse primer (exon 10)	ACCGTCAAGTCTGCAAGGTC
	5'FAM/3'BHQ1-probe (exon 10)	TCTGGAGGAGGCAAGTCATT
GAPDH	forward primer (exon 3)	CAACGGATTTGGTCGTATTGG
	reverse primer (exon 2/3)	TGATGGCAACAATATCCACTTTACC
	5'VIC/3'TAMRA-probe (exon 3)	CGCCTGGTCACCAGGGCTGCT

Supplementary Table 5. Taqman-based RT-qPCR and *SMN2*-specific primers and probes used to quantify mRNA levels of *SMN2*, STRN3 and *GAPDH* (Suplementary Fig. 4C)

RNA	MW	Sequence
ESE1	5032.9	5'-AAA AAG AAG GAA GG-3'
ESE2	5032.9	5'-AAA AAG AAG GAA GG-3'
ESE3	4130.3	5'-ACA UUC CUU AAA-3'
ESE3_TSL2	8687	5'-UCUCAU UCC UUA AAU UAA GGA GUA AG-3'
antisense TSL2	8640.9	5'-CUU ACU CCU UAA UUU AAG GAA UGU GA-3'
Exon 7	21099.6	5'-UAC AGG GUU UUA GAC AAA AUC AAA AAG AAG GAA GGU GCU CAC AUU CCU UAA AUU AAG GAG UAA G-3'
ISS-N2	14491.4	5'-CAC UAG UAG GCA GAC CAG CAG ACU UUU UUU UAU UGU GAU AUG GG-3'
TSTL4/6	14745.6	5'-AUA ACC UAG GCA UAC UGC ACU GUA CAC UCU GAC AUA UGA AGU GCU-3'
I7_c	12450.2	5'-CGU CAA GCC UCU GGU UCU AAU UUC UCA UUU GCA GGA AA-3'
TSL7	16129.5	5'-CUA GUC AAG UUU AAC UGG UGU CCA CAG AGG ACA UGG UUU AAC UGG AAU U-3'
GA	5064.9	5'-GAG AGA GAG AGA GA-3'
GU	4903.7	5'-GUG UGU GUG UGU GU-3'
STRN3 "ESE"	9745.9	5'-AAG AAG GAA CGA AAG GGG AAG AAA GGG G-3'

Supplementary Table 6. RNA sequences used for immobilization in surface plasmon resonance experiments on Biacore (Fig. 4b, 4C, 4D)

Ingredient	**µL/1 reaction**
5x transcription buffer (Roche Diagnostics, 11465384001)	2.5
4 rNTP mix (2.5 mM A, 2.5 mM C, 0.5 mM G, 0.5 mM U)	2.5
100mM DTT	1.25
10mM m7G(5′)P(5′)G-cap structure analog (New England Biolabs, S1407L)	0.624
RNase-In (Promega, N251B)	1
Water	1.126
^{32}P-UTP	1.5

Reagent	**Volume (µl)**
H_2O	8.15
cDNA template	1.5
10x PCR buffer (Applied Biosystems, R09952)	1.25
10mM dNTP mix	0.375
10pmol/µl primer F	0.375
10pmol/µl primer R	0.375
[α-^{32}P]dCTP	0.1
AmpliTaq DNA polymerase (AB, 100020478)	0.375
Total:	**12.5**

Program:

Step	Temp (°C)	Time (mm:ss)
1	94	03:00
2	94	00:34
3	55	00 :50
4	72	00 :36
5	Go to step 2, 25 times	
6	72	05 :00
7	4	For ever

Primer:

T7_fw	Tacttaatacgactcactataggctagcctcg
Ex8_pCI-neo_rv	Aagtacttacctgtaacgcttcacattccagatctgtc
Ex7_pCI-neo_rv	aagtacttac tccttaatttaaggaatgtgagcaccttcc

Supplementary Table 7. *In vitro* transcription buffer and radioactive PCR protocol for in vitro transcription assay in HEK293 cells (Figure 2G)